DEPARTMENT OF ENERGY

Final Report DOE/PC/92529--T13

SEPTEMBER 30, 1996

Project DE-FG22-92PC92529

Transient Studies of Low Temperature Catalysts for Methane Conversion

directed by

Eduardo E. Wolf
Professor
Chemical Engineering Department
University of Notre Dame
Notre Dame, IN 46556

DISCLAIMER

TABLE OF CONTENTS

	PAGE
LIST OF TABLES	ii
LIST OF FIGURES	ii
1. ABSTRACT.	1
2. PROJECT OBJECTIVES.	3
3. INTRODUCTION.	3
3.1 GENERAL INTRODUCTION.	3
3.2 INTRODUCTION TO EACH REACTION PATHWAY	4
3.2-1 PARTIAL OXIDATION OF METHANE TO FORMALDEHYDE ON VPO CATALYSTS.	4
3.2-2 METHANE OXIDATIVE COUPLING ON $Li/LaNiO_3$ CATALYSTS.	5
3.2-3 PARTIAL OXIDATION OF METHANE TO SYNGAS ON Rh CATALYSTS.	6
4. TECHNICAL STRATEGY.	7
5. EXPERIMENTAL APPARATUS AND PROCEDURE.	7
5.1 APPARATUS.	7
5.2 CATALYTIC ACTIVITY MEASUREMENTS.	8
5.2-1 PARTIAL OXIDATION OF METHANE TO FORMALDEHYDE ON VPO CATALYSTS.	9
5.2-2 METHANE OXIDATIVE COUPLING ON $Li/LaNiO_3$ CATALYSTS.	10
5-2.3 PARTIAL OXIDATION OF METHANE TO SYNGAS ON Rh CATALYSTS.	11
5.3 CATALYST CHARACTERIZATION.	11
5.4 TRANSIENT STUDIES.	12
6. DATA REDUCTION, INTERPRETATION AND ANALYSIS.	13
7. RESULTS AND DISCUSSION.	13
7-1 PARTIAL OXIDATION OF METHANE TO FORMALDEHYDE ON VPO CATALYSTS.	13
7-2 METHANE OXIDATIVE COUPLING ON $Li/LaNiO_3$ CATALYSTS.	28
7-3 PARTIAL OXIDATION OF METHANE TO SYNGAS ON Rh CATALYSTS.	40
8. CONCLUSIONS.	48
9. REFERENCES.	50

LIST OF TABLES

Page

Table 1 Assignments of the FTIR bands to vibration modes in the region (500-1500 cm^{-1}) for some of the unsupported samples. 18

Table 2. XPS intensity ratio I_{Li}/I_V for the Li1s and V2p3/2 peaks in the unsupported catalysts. 19

Table 3. Percentage of the different O_2 isotopes in the outlet (referred to the total oxygen present in the flow) after 4 min of $^{18}O_2$ exchange on various supported catalysts at 923 K. 20

LIST OF FIGURES

Page

Figure 1: Schematic diagram of the apparatus. 8

Figure 2: Schematic diagram of the membrane reactor. 10

figure 3. XRD diffraction pattern of VPO-u. 14

Figure 4a: FTIR spectra for several samples in the region 3750-2900 cm^{-1}. 15

Figure 4b. FTIR spectra for several samples in the region 1750-1550 cm^{-1}. 16

Figure 5: FTIR espectra for several unsupported samples in the region (1500-500 cm^{-1}). 17

Figure 6: CH_4 conversion (%) as a function of temperature for several unsupported catalysts (conditions as indicated in experimental section). 20

Figure 7: HCHO selectivity(%) as a function of CH_4 conversion(%) for the same catalysts of fig. 6. 21

Figure 8: CH_4 conversion (%) as a function of temperature for several supported catalysts (conditions as indicated in experimental section). 21

Figure 9: HCHO selectivity(%) as a function of CH_4 conversion (%) for the same catalysts of fig.8. 22

Figure 10: Comparison of the HCHO selectivity vs CH_4 conversion curves in double bed and single bed configurations at two different flow rates (conditions as indicated in experimental section). 23

Figure 11. $^{18}O_2$, $^{16}O_2$ and $^{16}O^{18}O$ concentrations in the effluent when a $^{18}O_2$ step in He is fed through a Li-VPO/SiO_2 at 923 K. 24

Figure 12. XRD patterns of unpromoted and Li promoted $LaNiO_3$. 29
Figure 13. CH_4 conversion and C_2 selectivities vs reaction temperature during OC reaction at different Li loadings. 30
Figure 14. CH_4 conversion and C_2 selectivities vs reaction temperature on $LaNiO_3$ catalyst with different Ni/La ratio. 31
Figure 15. Pulses of methane over a $LaNiO_3$ catalsyst at 700°C 32
Figure 16. CH_4 pulses with different O2 concentration on $LaNiO_3$ at 550°C. 33
Figure 17. CH_4 pulses with different O2 concentration on 2.5% $Li/LaNiO_3$ at 700°C.
Figure 18. CO_2 signal during CH_4 and O_2 pulses on 2.5% $Li/LaNiO_3$, fresh and CO_2 treated at 650°C. 34
Figure 19. C_2H_6 and O_2 pulses with different O_2 concentration at 650°C.a- CO_2 signal, b- O_2 signal. 35
Figure 20. $^{18}O_2$ isotopic exchange at 700°C on $LaNiO_3$ and 7.5% $Li/LaNiO_3$. 36
Figure 21. $^{18}O_2$ and $^{16}O^{18}O$ signals during a TPIE experiment. 37
Figure 22.Methane 13 isotopic switch in the presence of Ar and oxygen on $LaNiO_3$ catalyst at 650°C. 38
Figure 23. Methane and oxygen conversion versus temp. for $LaNiO_3$, $LaCoO_3$, $LaRhO_3$. 41
Figure 24. Methane conversion and C_2 selectivity for Li promoted catalysts. 41
Figure 25. Selectivity for the $LaRhO_3$ catalysts. 43
Figure 26. Conversion and selectivity on a Rh/TiO_2 catalyst as a function of residence time. 44
Figure 27 Methane and oxygen conversion versus residence time in a fast flow membrane reactor. 45
Figure 28. Pulses of CH_4/O_2 mixtures over the $Li/LaRhO_3$ catalyst. 46

1. ABSTRACT

The oxidative conversion of methane was studied in catalysts containing a metal oxide function and another oxygen bearing compound. The selectivity obtained depended on the type of metal oxide, the second component, and the promoter used. Thus, the reaction pathway for oxidative methane conversion could be directed towards the formation of formaldehyde (FA), C_2 hydrocarbons, or to synthesis gas (syngas: H_2, CO) production. Due to the differences in reaction conditions, each pathway was studied separately.

The first catalytic system selected was the partial oxidation of methane to formaldehyde on $VOPO_4$ (VPO) catalysts. The unpromoted catalyst yielded low selectivity which increased upon Li promotion. The catalytic results clearly show that the Li cation improves the FA selectivity on VPO phases. The conversion and selectivity obtained depended on the method of introduction of the Li promoter. Characterization and transient studies showed that to obtain an active and selective catalyst, Li^+ has to be intercalated between the layers of $VOPO_4*2H_2O$ which upon calcination forms the active phase. While the results regarding the role of Li could be significant in designing other catalysts for this reaction, the Li/VPO catalyst exhibited the type of low selectivity at low conversion characteristic of other catalysts reported for this reaction in the literature. For this reason no further studies of this reaction pathway were conducted, and attention was focused on the oxidative coupling reaction.

Studies on double oxides of metals (Co, Ni and Rh) and lanthana (La_2O_3) demonstrated that in fact the combination of these two catalytic functions yielded catalysts that operated at lower temperatures. The methane-metal oxide interactions however, were too strong, and the unpromoted catalysts exhibited low or no C_2 selectivity during the oxidative coupling of methane. The $LaRhO_3$ catalyst, however, was very selective to synthesis gas production instead of total combustion. The C_2 selectivity increased dramatically upon promotion with Li, particularly for the $LaNiO_3$ catalyst. Hence the oxidative coupling of methane was studied on $Li/LaNiO_3$ using transient techniques. For a $5\%Li/LaNiO_3$ catalyst the selectivity towards C_2 products increased from 2% up to 75% at 750°C. The increase in selectivity was achieved, however, at the expense of higher temperatures, hence the intended low temperature reactivity was not realized in the $Li/LaNiO_3$ catalyst. Transient experiments and isotopic exchange experiments on unpromoted and Li promoted $LaNiO_3$ catalysts indicate that the presence of lithium significantly decreases the oxygen exchange capabilities of $LaNiO_3$ by blocking oxygen exchange sites which may also be responsible for the total oxidation of methane. While the transient studies clearly revealed the role of Li, the yields attained in the Li promoted $LaNiO_3$ catalyst were similar to results reported for other Li promoted catalysts reported for this reaction in the literature. Hence attention was directed to the one outstanding

result obtained, namely that the $LaRhO_3$ catalyst exhibited high selectivity to syngas production at relatively low temperatures.

Results with $LaRhO_3$ showed that this catalyst exhibited an unusual selectivity for synthesis gas production. The $LaRhO_3$ catalyst retained its high selective for syngas production even in the presence of Li. Furthermore, this catalyst ignited at relatively low temperatures to a high conversion state in a methane-oxygen undiluted feed. This allowed one to study the reaction at low CH_4/O_2 ratios in a fixed bed reactor. *Studies of a 3% Rh supported on TiO_2 catalyst showed that the ignition temperature was even lower than on the $LaRhO_3$ catalysts. Furthermore, it was fund that the Rh/TiO_2 catalyst operated autothermally in an undiluted feed at millisec residence times.* ***These are in fact the most significant results of this work.*** These results lead to the development of a fast flow membrane reactor which by keeping the methane and oxygen feeds separated, can be operated safely under the partial oxidation conditions. The results in the membrane reactor were similar or better than in the fixed bed studies. *These results have open up the possibility of converting methane to syngas in an autothermal mode at low temperature using low reactor volumes. This process has a significant commercial possibilities and further scaling up studies must be conducted to realize this potential.*

2. PROJECT OBJECTIVES

The objective of this project is to use transient techniques to study gas surface interactions during the oxidative conversion of methane. Two groups of catalysts were studied: a double oxide of vanadium and phosphate or VPO, and double oxides of Ni, Co and Rh and lanthana. The objective of the studies involving the VPO catalyst was to understand gas-surface interactions leading to the formation of formaldehyde. In the second group of catalysts, involving metallo-oxides, the main objective was to study the gas-surface interactions that determine the selectivity to C_2 hydrocarbons or synthesis gas. Transient techniques were used to study the methane-surface interactions and the role of lattice oxygen. The selection of the double oxides was made on the hypothesis that the metal oxide would provide an increase interaction with methane whereas the phosphate or lanthanide would provide the sites for oxygen adsorption. The hypothesis behind this selection of catalysts was that increasing the methane interaction with the catalysts would lower the reaction temperature and thus increase the selectivity to the desired products over the total oxidation reaction. In both groups of catalysts the role of Li as a modifier of the selectivity was also studied in detail.

3. INTRODUCTION

3.1 GENERAL INTRODUCTION.

The oxidation of methane to C_1 oxygenates or C_2 hydrocarbons has attracted the attention of many research groups over the last ten years due to its potential to transform the extensive reserves of natural gas into building block molecules for the petrochemical industry (methanol, formaldehyde, or ethylene). These efforts have been hampered by the lack of reactivity of methane compared to the intended products which are readily oxidized to CO_2 in the presence of oxygen. The two reaction pathways selected have been extensively studied, and a book summarizing the state of the art of the oxidative conversion of methane has been published (1).

In the case of the partial oxidation of methane to oxygenates catalytic studies have shown (2) disappointingly low conversions (up to 7 %) with selectivities decreasing drastically with increasing conversions (from 40 % selectivity at 1% methane conversion to less than 5% selectivity at 5% methane conversion). Nonetheless this pathway is attractive because the products can be easily separated from methane which can be recycled back to the reactor. Consequently, under these conditions, a low conversion but selective process could be feasible. This reaction pathway was studied on a $VOPO_4$ (VPO) catalysts because P has been described as a promoter for the formaldehyde yield when added to metal oxides. Studies involving the VPO catalysts constitute one of the main reaction pathways studied in this project.

The second reaction pathway studied was the oxidative coupling of methane on metallo oxide catalysts. This reaction has received considerable attention in the last ten years (1). The main result that has emerged from previous studies is that, as in the case of the partial oxidation to oxygenates, the selectivity to C_2 products decreases with conversion. In this case however, selectivities in the order of 60-70% can be achieved at conversions ranging from 20-30%. In hundreds of catalysts studied it has been found that the yield is limited to about 25% which is not sufficient for the process to be commercially feasible. The main limitation in this case are the separation processes needed to separate the C_2 products from unconverted methane. These are cryogenic processes, involving compression and low temperatures, which are very costly. Thus to increase the C_2 selectivity at higher conversions is one of the main objectives of research in this area. One route to improve selectivity is to decrease the reaction temperature so that the products generated are not combusted before emerging from the reactor. Increasing the methane-surface interactions is one of the routes that can lead to lower reaction temperatures, hence the selection of the metallo oxide catalysts, since metals are known to interact with methane. Of the three metallo-oxide catalysts studied, $LaCoO_3$, $LaNiO_3$ and $LaRhO_3$, the $Li/LaNiO_3$ was the most selective catalyst to C_2 hydrocarbons. Hence the second major effort of this project focused on studying the role of Li promotion leading to high C_2 selectivity using steady state and transient techniques.

The partial oxidation of methane to synthesis gas is also a reaction of industrial interest since, upon further processing, it can lead to liquid products such as methanol or hydrocarbons. Current syngas production is achieved via methane steam reforming, which is an endothermic reaction and requires energy consumption. Syngas production constitutes a significant fraction of the cost (~ 30%) of liquids from syngas. The third section of this study focused on the partial oxidation of methane to syngas on the Rh metallo-oxide catalysts and its supported form. Rh exhibited unusual selectivity to syngas hence its selection for these studies. To achieve this in a safe and efficient manner a fast flow membrane reactor was developed which yielded the most interesting results of this work.

Since in each case the catalyst was different, each section of this report is divided into the three reaction pathways studied: 1) partial oxidation to formal aldehyde on VPO catalyst, 2) oxidative coupling of methane on a $Li/LaNiO_3$ catalyst, and 3) partial oxidation of methane to syngas on a Rh catalyst. In each case, transient techniques were used to study the gas-surface interactions to determine the role of each catalysts' component on the activity-selectivity results obtained.

3.2 INTRODUCTION TO EACH REACTION PATHWAY.

3.2-1 PARTIAL OXIDATION OF METHANE ON VPO CATALYSTS.

Several reviews have been published about the partial oxidation of methane (1-4). Among the best catalysts reported to oxidize selectively methane to formaldehyde are MoO_3/SiO_2 (5-8), V_2O_5/SiO_2 (9), Bi_2O_3/SnO_2 (10) and FeNbB-O (11). High formaldehyde

(FA) selectivity is only obtained at low CH_4 conversions (< 2%) whereas at higher conversions the total oxidation products (CO and CO_2) become predominant. The addition of various promoters to the above mentioned catalysts have resulted in an increase of the FA yield. Thus, P atoms has been described as a promoter for the FA yield when added to metal oxides systems (12, 13). As vanadyl phosphate (VPO) phases are good partial oxidation catalysts for the conversion of butane to maleic anhydride reaction (14), it was deemed interesting to explore its behavior during methane oxidation. Among the metal phosphates, $VOPO_4$ has been reported as one of the most active and selective (15). The goal of this work was to investigate the effect of the addition of Li promoter on the FA yield of VPO phases.

The VPO phase used as starting material was the $VOPO_4*2H_2O$. This V^V compound can be described as layers of VO_6 octahedra sharing the four equatorial O atoms with PO_4 groups in the ab plane (14, 16). The water molecules are located between the $VOPO_4$ layers. The water is driven off the inter laminar space at low temperatures (< 100 °C) yielding α_I-$VOPO_4$ (17). The α_I-$VOPO_4$ can be described as $VOPO_4$ layers lying in the ab plane as well, but the VO_6 octahedra are also sharing the axial O atoms with other V atoms forming chains of octahedra running along the c axis (18-20). α_I-$VOPO_4$ is thermally stable until around 993 K, where it undergoes an irreversible transformation to the α_{II} phase, which has basically the same layered structure as the α_I-phase, but it differs in the relative position of the vanadyl group (V=O) as compared to the tetrahedra.

Li^+ has been studied as a promoter of alkali oxides during the oxidative coupling of methane but it has not been reported as a promoter in the selective oxidation methane to obtain FA. In this work, the Li cation was added to the VPO system following two different procedures: a) the intercalation of Li cations between the layers of $VOPO_4*2H_2O$ through a redox intercalation process, and b) the coprecipitation of a Li compound with a VPO phase. The intercalation method has the potential advantage that it may result in the dispersion of the Li cations on the VPO phase surface when the catalyst is calcined. XRD, FTIR and XPS characterization were carried out to understand the effect of Li on both the structural and catalytic properties of the VPO catalysts. In addition, double bed experiments under different space velocities were performed, in which a SiO_2 supported VPO catalyst was placed upstream of a Li/SiO_2 catalyst in order to determine whether the Li phase is able to transform selectively the intermediates created by the VPO phase. $^{18}O_2$ isotopic exchange experiments were also carried out to detect the different capabilities of various catalysts to exchange gas phase and lattice oxygen, since this can be related to differences in the surface state.

3.2-2. METHANE OXIDATIVE COUPLING OVER $Li/LANiO_3$.

The most active catalysts for the formation of ethane and ethylene during oxidative coupling of methane are reducible metal oxides, rare-earth metal oxides, or the oxides of alkali and alkaline earth metals (1). The main issues that have to be better understood to improve higher

hydrocarbons yields are the methane surface interactions, the type of oxygen species responsible for methane activation, the role of unselective oxidation reactions, and the influence of different promoters on the activity of the catalysts. In general, it has been found that reducible metal oxides are involved in a redox cycle similar to the Mars-van Krevelen mechanism (21), with lattice oxygen involved in the process. In the case of alkali promoted transition metal oxides and rare-earth metal oxides, different forms of oxygen on the surface are the sites responsible for hydrogen abstraction from methane to form a free methyl radical that dimerizes in the gas phase (22-26). The pathway for the formation of CO_2 can involve direct oxidation of methane, or the combustion of C_2 products. To improve C_2 yield is necessary to understand the nature of the methane surface interactions, the identification of the oxygen species responsible for methane activation, the role of non-selective oxidation reactions, and the influence of different promoters on the activity of the catalysts.

The hypothesis behind the selection of the metallo-oxide catalyst is that the metal oxide will provide sites for the interaction of methane with the surface which will lead to a lower reaction temperature. The other oxide will provide the pathway to supply oxygen to the surface. The metal oxides chosen, Ni, Co and Rh have proven to be able to activate methane at much lower temperatures than those usually used in the oxidative coupling reaction (27). The other oxide selected was lanthana since this oxide is known to supply oxygen from the lattice for interaction with surface species.

This section of the study focused specifically on the effect of Li on $LaNiO_3$, because this was the most selective of the three metallo-oxides for oxidative coupling. Lithium has shown to be an effective promoter in alkaline oxides such as TiO_2 and La_2O_3 catalysts (28-30). The effect of lithium promotion on $LaNiO_3$ was studied using transient techniques to determine the role of lattice oxygen in the formation of C_2 products.

3.2-3. PARTIAL OXIDATION OF METHANE TO SYNGAS ON Rh CATALYSTS.

The other reaction pathway studied was the conversion of methane to synthesis gas. Preliminary studies conducted on the double oxides of Ni, Co and Rh and La showed that although the reaction temperature was lowered, the C_2 selectivity of these catalysts was very low except for the $Li/LaNiO_3$ catalyst. The $LaRhO_3$ catalyst, however, exhibited an unusually high selectivity to CO and a very low reaction temperature. Since this material required a significant amount of Rh it was decided to study the activity and selectivity of Rh supported on several supports and found that Rh/TiO_2 was the most selective and stable catalyst. The study included two important modifications of previous work done by Schmidt and coworkers (31) on the partial oxidation of methane to syngas on a Rh supported on a monolith catalyst. First, in order to be able to operate in a safe range of conditions the methane and oxygen feeds were separated by a porous membrane tube. Second the reaction was conducted on a powder catalyst at temperatures much lower than those used in monolith catalysts. In this case the emphasis

was to evaluate the performance of the Rh catalyst at very fast flow-low residence time. The results obtained in the last part of this work lead to the development of a new fast flow- millisec residence time membrane reactor for the conversion of methane to syngas in an almost autothermal reaction. This result is the most significant of the study since it has potential for industrial application.

4. TECHNICAL STRATEGY

The basic strategy followed in this work was to use transient techniques to understand gas-surface interactions. It was expected that this knowledge would permit to design more selective catalysts for the oxidative conversion of methane. The strategy evolved with the results obtained. The basic hypothesis that metallo oxide catalyst will increase methane-surface interactions and lower the reaction temperature was essentially valid in both VPO and $LaMO_3$ catalysts(M=Co,Ni,Rh). The selectivity of these catalysts to the intended product, however, was very low except when a Li promoter was added. Li made the catalysts more selective towards formaldehyde in the case of VPO, and to C_2 hydrocarbons in the case of the $LaNiO_3$. Consequently in the partial oxidation to formaldehyde and methane oxidative coupling, the transient studies focused on determining the effect of the Li promoter on improving the VPO and $LaNiO_3$ selectivity.

Basically in the first two sections of this work the following steps were followed:

a) Evaluate the activity and selectivity of the unpromoted catalysts (VPO and $LaMO_3$).

b) Conduct bulk characterization by x-ray diffraction.

c) Study the effect of the Li promoter on activity and selectivity.

d) Conduct transient studies to evaluate the effect of the promoter on the effect of methane and oxygen interaction with the surface.

e) Conduct surface characterization (XPS, IR) of the most selective catalysts.

In studies related to conversion of methane to syngas, the main emphasis was to develop a membrane reactor under fast flow conditions. In this case the catalysts' formulation was fixed and the strategy was to determine the effect of the reaction operating conditions and reactor configuration on the selectivity to CO and H_2.

5. EXPERIMENTAL APPARATUS AND PROCEDURE

5.1 APPARATUS.

A schematic diagram of the apparatus used is shown in figure 1. It consists of a tubular reactor which can be used for steady state activity measurements as well as transient experiments. Electronic flow controllers (Brooks Instruments Co.) and programmable

temperature controller (Omega 2012) mantained these variables at specified values during the experiment. These were in term interfaced to a computer using a special software (Lab. View) which permitted to specify the type of experimental protocol to be used . A six port sample valve as well as a four way valve were used to perform transient experiments. The transient experients consisted in sending pulses or step changes in the concentration of one of the reactants into a carrier gas (He) that passed over the catalysts bed. A line was connected to isotope containers for their use in isotopic exchange experiments.

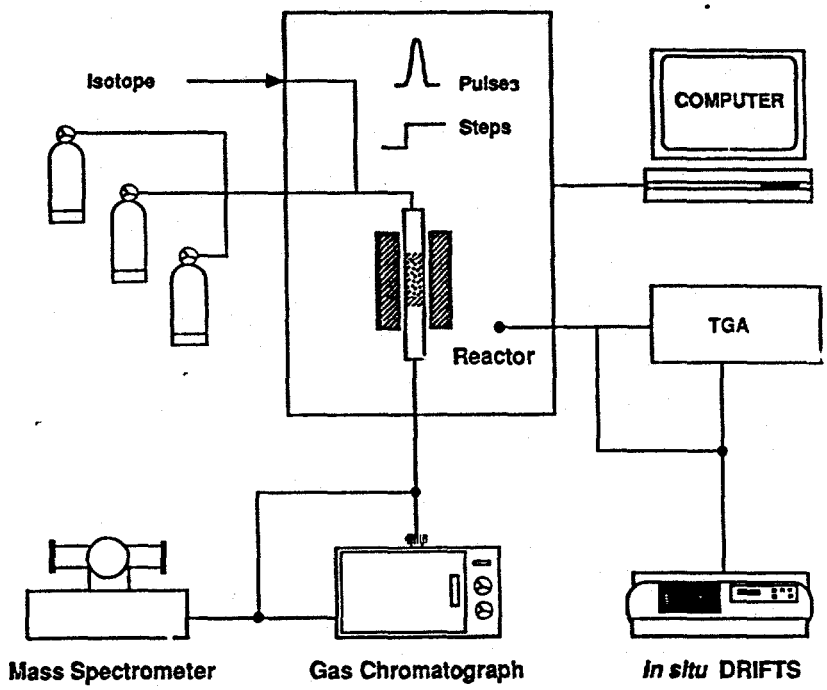

Fig. 1 . Schematic diagram of the equipment.

The effluent stream was analyzed via gas chromatography, or mass spectrometry in the case when isotopes were involved. The amount of catalyst, flow rates used, and analytical system used depended on the reaction under study thus such conditions are specified separately in each case. In addition of controlling the flows for the reactor, the control panel allow to direct these flows to an on-line infrared reactor (DRIFTS) or to a TGA.

The gases were ultrahigh purity quality and they were used as delivered without further purification (He 99.995% (Mittler Supply Inc.), CH_4 99.99% (AGA) and O_2 99.99% (Linde Specialty Gases).

5.2 CATALYTIC ACTIVITY MEASUREMENTS.

Steady state reaction studies were carried out at atmospheric pressure in a 10 mm I.D. quartz fixed-bed reactor. Immediately downstream the catalytic bed, the inner tube diameter was narrowed down to 3 mm I.D. to decrease the residence time in the post reactor volume. A

K-type thermocouple was introduced in a 9 mm O.D. concentric quartz tube to the reactor walls which fits tightly and reduces the residence time in the prereactor volume. The gases flow into the catalyst bed in the narrow space between the inner and the outer quartz tubes. The bottom part of the thermocouple well lies on the catalyst bed so that its temperature can be measured accurately (28).

5.2-1. PARTIAL OXIDATION OF METHANE TO FORMALDEHYDE ON VPO CATALYSTS.

The catalytic runs during the partial oxidation to formal aldehyde studies were performed with 0.2 g of catalyst at 26 cc/min total flow rate, CH_4/O_2= 3.39, P'=(CH_4+O_2/total flow rate) = 0.6 and GHSV (gas hourly space velocity) = 0.130 l(STP)*s^{-1}*g $cat.^{-1}$. Blank reactor runs were carried out and no conversion was detected in the temperature ranges used in this work. Gas phase reaction were more important at more drastic conditions: total flow rate 26-100 cc/min, CH_4/O_2= 2, P'=0.72 and at temperatures higher than 1130 K.

The effluent gases composition was measured on line at the reactor effluent using a HP5710A gas chromatograph (GC) equipped with a thermal conductivity detector. All the lines from the reactor to the GC were heated above 373 K to avoid water and FA condensation. A 3 m HayesSepT and 3 m HayesSepQ columns connected in series were used to analyze O_2, CH_4, CO_2, C_2H_6, C_2H_4, HCHO and H_2O. A 3m Carbosphere column was utilized to analyze O_2, CO, CH_4 and CO_2.

In addition to the activity studies using a single bed, experiments were also conducted using a double bed with two separate catalyst functions in the reactor. The upstream bed was made of a VPO/SiO_2 catalyst (0.2g) and the downstream bed separated by quartz wool contained a Li/SiO_2 catalyst (0.05g). Two runs were carried out at 848 K at two different GHSV values referred to VPO/SiO_2 bed: 0.61 l(STP)s^{-1}g $cat.^{-1}$ and 0.13 l(STP)s^{-1}g $cat.^{-1}$ (122 cc/min and 26 cc/min, respectively). The feed concentration for each specific run were P'=0.50 and CH_4/O_2=3.13 for the 122 cc/min run and P'=0.57 and CH_4/O_2=3.39 for the 26 cc/min run .

In both steady state and double bed runs C or O mass balance were carried out on the basis of C or O atoms in the outlet flow compared to C or O atoms in the outlet . The balance was always closed with less than a 5 % of difference.

5.2-2. METHANE OXIDATIVE COUPLING ON Li/$LANiO_3$ CATALYSTS.

The same reactor as described previously for the partial oxidation to formal aldehyde, were used in studies of methane oxidative coupling and methane partial oxidation to syngas. A typical set of operating conditions during activity measurements during oxidative coupling experiments were as follows: atmospheric pressure, 50 mg of catalyst, total flow rate of 100 cc/min (STP), and methane/oxygen mole ratio of 4. In some cases, experiments were repeated twice to check for the reproducibility of the results. Reactants were diluted in helium, so the

reactants partial pressure, $P^*=(P_{CH4}+P_{O2})/P_{tot}$, was equal to 0.4 to minimize gas phase reactions (26).

Effluent gases were analyzed by an on-line gas chromatography (GC), equipped with a TCD and FID detectors. Two chromatography columns operated in parallel allowed for the sufficient separation of effluent gases: a HayeSep Q polymer-packed column for the separation of CO_2, C_2H_4, C_2H_6, C_3H_6, and C_3H_8, and a Carbosphere-packed column for the separation of H_2, O_2, CO, CH_4 and CO_2. An ice trap was placed at the reactor exit in order to remove water from the reaction products. In most of the experiments closures on carbon mass balances were reached within 2-4 %.

5.2-3. PARTIAL OXIDATION OF METHANE TO SYNGAS ON Rh CATALYSTS.

Similar analysis and reactor as described above was used in the initial studies of methane conversion to syngas on Rh catalysts. In this case, however, very little C_2 selectivity was detected and the emphasis focused on selectivity to CO and H_2. The reaction conditions however differed significantly. In this case no He diluent was used leading to high methane conversion. After ignition, the heat evolved resulted in an autothermal operation in the 500-600°C range. The low methane to oxygen ratio however, could lead to unsafe operation since a hot spot could develop leading to an explosion. To avoid the explosive conditions a membrane reactor was developed. A schematic diagram of the reactor is shown in figure 2.

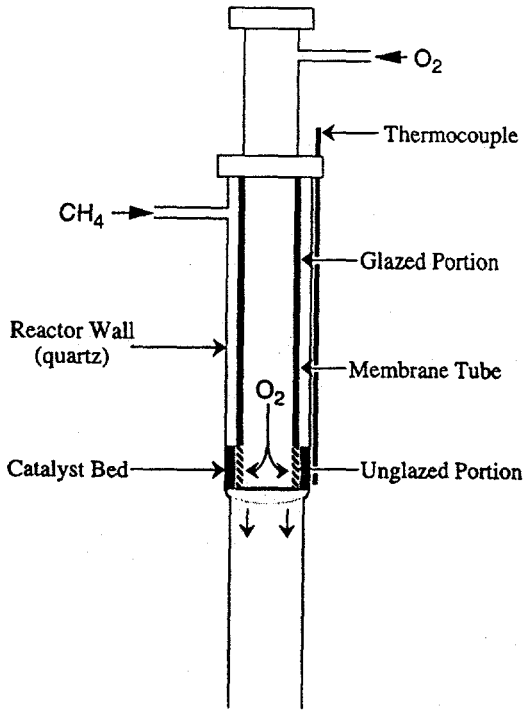

Fig. 2 Schematic diagram of the membrane reactor.

In this case the oxygen and methane are fed separately so that if a flame developed, it could not propagate into any of the two streams. The same feed and temperature control system used for the fixed bed operation were also used in the operation of the membrane reactor. Higher flow rates, however, were used in studies involving a millisec membrane reactor.

5.3 CATALYST CHARACTERIZATION.

The following characterization techniques were common to the three reaction pathways studied.

X-Ray Diffraction. X-Ray diffraction patterns were measured in a Diano XPG-2X diffractometer. The runs were made with a scanning speed of 1.0 °/min and a detector slit width of 0.2 °. The radiation used was CuKa and the source voltage and amperage were 45 kV and 30 mA, respectively. The samples were supported on an adhesive tape mounted on glass slides.

BET surface area measurements. These were measured in a Quantachrome QS-8 unit using the flow adsorption method with nitrogen as the adsorbing gas and ultra high purity helium as a carrier.

FTIR measurements. The FTIR spectra were obtained in a Galaxy Series FTIR 6020 spectrometer (Mattson Instrument) purged with dried air and equipped with a MCT detector. The spectrometer resolution was set at 4 cm^{-1}. Pellets were used to carry out the measurements and they were prepared by diluting the samples in KBr powder and pressing the resulting mixture.

X-Ray Photoelectron Spectroscopy. The photoelectron spectra (XPS) were recorded with a Fisons ESCALAB MK11 2000R spectrometer provided with a hemispherical electron analyzer and a Mg anode X-ray exciting source (MgK=1253.6 eV). The samples were pressed into small aluminum cylinders and then mounted on a rod placed in the pretreatment chamber of the spectrometer. The samples were pumped to ca. 10^{-6} Torr (1Torr=133.33 Nm^{-2}) before they were transferred into the analysis chamber. The residual pressure in this chamber was maintained below $3*10^{-9}$ Torr during data acquisition. A 20 eV energy regions of the photoelectrons of interest at a pass energy of 20 eV were chosen for each sample. Each spectral region was signal averaged for a number of scans to obtain good signal to noise ratios. A binding energy (BE) of 284.9 eV corresponding to the C1s peak was used as an internal standard.

5.4 TRANSIENT STUDIES.

The following transient techniques were common to the three reaction pathways studied.

Pulse experiments. During transient pulse experiments involving methane and oxygen both gases were diluted in helium before entering a loop of a GC sampling valve. The ratio of methane to helium in the pulse could be varied depending on the experiment.

Isotopic $^{18}O_2/^{16}O_2$ exchange experiments. These were conducted in the 600°C to 750°C temperature range using 20 mg of catalyst. Oxygen ($^{16}O_2$) flow rate was adjusted at 2 cc/min. Gases were diluted in helium, so the total flow rate was 60 cc/min. At time zero a step change in the concentration of a mixture containing the $^{18}O_2$ isotope is introduced over the catalyst over a period of about 7 minutes. The effluent gases were analyzed by a UTI 100C quadrupole mass spectrometer with a fast response sample introduction system. The signals for $^{16}O_2$ (referred hereafter as oxygen or O_2), $^{18}O_2$ isotope, and $^{16}O^{18}O$ scrambled oxygen are used to determine the amount of isotope exchanged as well as its mobility in the lattice (32,33).

Temperature programmed isotopic exchange (TPIE). This technique introduced in our laboratory, has proven to be an effective tool in the investigation of the lattice oxygen pathways during oxidation reactions (32). The $^{18}O_2$ isotope is first exchanged with O_2 from the lattice as described above. After the initial exchange, the reactor is brought to room temperature, and a flow of the oxygen and helium is introduced over a sample while the temperature program is started. In this study, the oxygen flow rate was fixed at 2 cc/min while the total flow was maintained at 60 cc/min. Of interest is to follow the signals of $^{18}O_2$ and $^{16}O^{18}O$ species as a function of temperature. The initial exchange of the $^{18}O_2$ with the lattice oxygen allows the TPIE experiment to be performed with significant economy in the isotope use.

$^{18}O_2$ isotopic oxygen was supplied by Isotec Corp. (95 % purity), and helium was used as a carrier gas. To dilute the oxygen isotope and prevent its fast depletion, it was transferred to an evacuated cylinder were it was pressurized with helium.

6. DATA REDUCTION, INTERPRETATION AND ANALYSIS.

The results presented in this report are in terms of methane conversion and selectivity. These were obtained from gas chromatographic data, which was converted to concentrations after calibration. Calibrations were periodically checked to insure reproducibility. Methane conversion (%) was defined as the sum of C atoms present in the products of the outlet*100 divided by the C atoms in the CH_4 inlet. The selectivity for every product was expressed as % of product (P_i), and it was calculated as C atoms in the outlet products (P_i) divided by C atoms converted. In the case of methane conversion to syngas, the H_2 selectivity was defined as the amount of H_2 product divided by the amount of hydrogen converted from methane. The other product, water, was trapped at the reactor effluent to prevent interference with the GC analysis.

During transient experiments the signals recorded were those obtained from the mass spectrometer . The signal corresponding to each mass was plotted directly in terms of a relative signal instead of absolute concentration values.

The signals from the characterization instruments (XRD, XPS, IR) were recorded directly as described in each case without further data processing.

7. RESULTS AND DISCUSSION

7-1.PARTIAL OXIDATION OF METHANE TO FORMALDEHYDE ON VPO CATALYSTS.

CATALYSTS PREPARATION.

a) Preparation of unsupported catalysts . The $VOPO_4*2H_2O$ was prepared following the procedure described by Ladwig et al. (20). A given amount of V_2O_5 (Aldrich) (12 g) was refluxed overnight with 65 ml of H_3PO_4 (85%) (Fisher Chemical) and with 240 ml of distilled water. The precipitate was filtrated and washed with distilled water; and dried at 473 K in air for 4 h and stored in air. This product was amorphous when analyzed by XRD. Then, it was re-crystallized by dissolving it in distilled water. The excess of water was evaporated until a few first like-lamina small crystals appeared in the solution. Then the solution was set aside for 24 h and the precipitate so formed was filtered, washed with water, dried in air at 473 K and stored in air. This uncalcined product was crystalline and its XRD corresponds to $VOPO_4*2H_2O$, and it is referred as VPO-u (the "-u" refers to uncalcined sample).

The intercalation of Li cations between the layers of $VOPO_4*2H_2O$ can be achieved by a redox process in which the salt of the cation and a reducing anion is dissolved in a suspension with $VOPO_4*2H_2O$ (17,34,35). The anion reduces the V^V to V^{IV} and the cation is driven to the interlayer space to balance the electric charge of the solid. A given amount of $LiI*3H_2O$ (Aldrich) was dissolved in the minimum quantity of distilled water. Then the $VOPO_4*2H_2O$ was added to the solution to attain a Li/V (at. ratio) = 1, and the suspension was stirred overnight at 323 K. Evidence that the redox process took place can be inferred from the release of I_2 violet gas (and I_2 crystals deposited on the walls of the flask), and also from the green color of the final precipitate which indicates a mixture of V^V (yellow) and V^{IV} (blue). The uncalcined precipitate was filtered, washed with n-butanol, dried in air at 473 K and stored in air yielding a solid referred as Li-VPO-u.

In the coprecipitation method, a given amount of Li_2CO_3 (Aldrich) was dissolved in a minimum amount of water. Then $VOPO_4*2H_2O$ was added until a Li/V (at. ratio) =1 was reached. The amount of water was enough to also dissolve the $VOPO_4*2H_2O$. The water was evaporated until dryness and all the components of the solution precipitated. The green precipitate so formed was dried in air at 473 K and stored in air and is referred as cop. Li-VPO-u.

b) Preparation of supported catalysts. $VOPO_4*2H_2O$ was deposited on SiO_2 by dissolving it in the minimum amount of boiling water, then adding SiO_2 (Cabosil EH-5) to the solution until the VPO phase represented 5% (taken as $VOPO_4*2H_2O$) of the total VPO/SiO_2 system. The water was evaporated under vigorous stirring until dryness. The green precipitate dried in air at 473 K and stored in air is referred as VPO/SiO_2-u. Redox intercalation of Li^+ in VPO/SiO_2 was accomplished by the redox process described above to prepare the unsupported

Li-VPO sample but applying it onto the VPO/SiO_2 solid instead. The procedure was as follows: a given amount of $LiI*3H_2O$ was dissolved in the minimum amount of water and then a certain quantity of the VPO/SiO_2 was added until the Li/V (at. ratio)=1, assuming that the VPO/SiO_2 was $VOPO_4*2H_2O$(5% weight)/SiO_2. This solution was stirred at 323 K overnight and some I_2 was released. The green precipitate was filtered, washed with n-butanol, dried in air at 473 K and stored in air and is referred as Li-VPO/SiO_2-u.

A silica supported Li phase was also prepared following the same steps than for Li-VPO/SiO_2, but without VPO addition. The $LiI*3H_2O$ was dissolved and the appropriate amount of SiO_2 was added to yield a Li(0.19% weight)/SiO_2. Thus, the Li/support ratio is the same than in the Li-VPO/SiO_2 sample. The solid is referred as Li/SiO_2-u.

Before loading the reactor, every precursor was calcined in air at 873 K. The catalysts so obtained are referred without the termination "u" i.e.: "VPO", "Li-VPO", etc. It is not expected that I^- species to be present on the surface of the calcined catalysts. I^- is a well known reducing agent and the calcination treatment should oxidize the remaining I^-, which has not been reacted with the V^V during the preparation, releasing I_2. Moreover, XPS analysis on calcined samples dit not show the presence of the I^- features.

CATALYST CHARACTERIZATION

X-Ray Diffraction. Figure 3 shows the X-Ray diffraction pattern of the unsupported VPO-u sample.

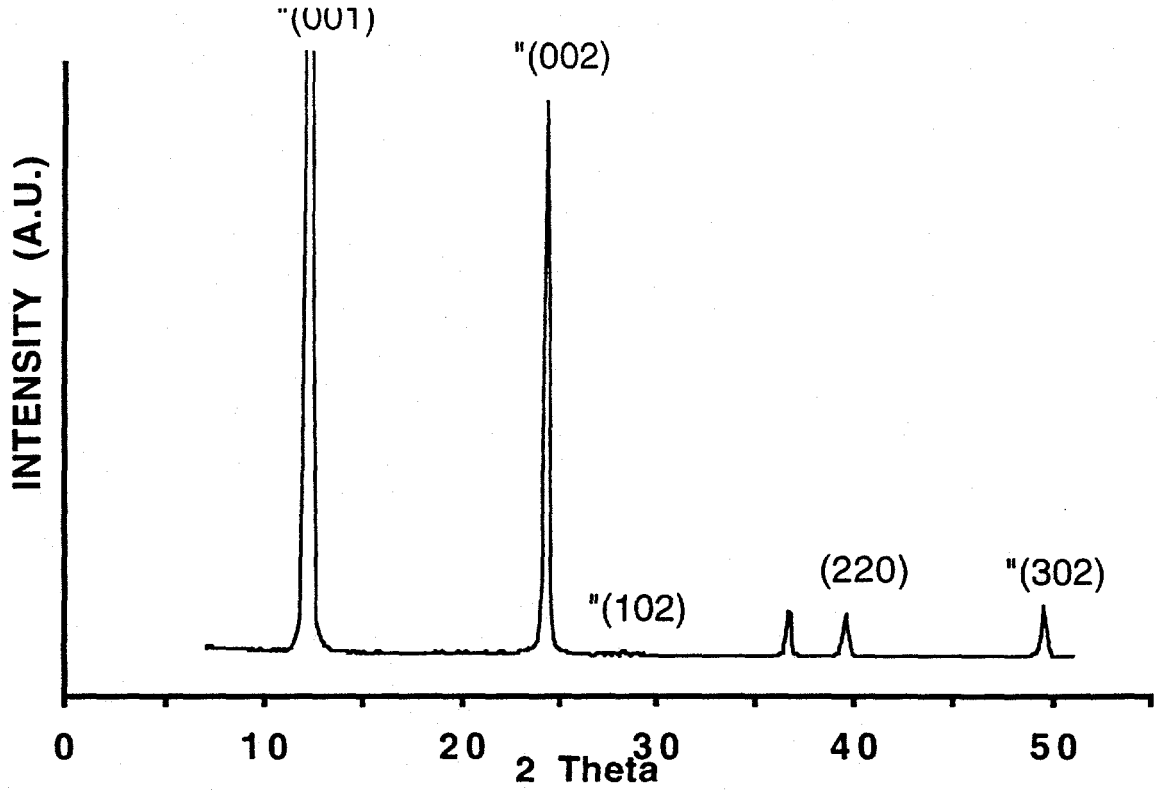

Figure 3: XRD diffraction pattern of VPO-u.

The pattern is very similar to the one reported in the bibliography for the $VOPO_4*2H_2O$ (17, 35). The assignment for the reflections agrees with that reported by Bordes et al. (14), except for the absence of the (101) reflection. The peak at d= 2.45 Å (2q=36.6) was not described by Bordes et al. (14) but it was present in the diffraction pattern reported by Antonio et al. (17) and Chauvel et al. (35) as $VOPO_4*2H_2O$. The other samples studied in this work did not show any diffraction lines. Thus, the remaining unsupported samples can be assumed to have a disordered structure, and the silica supported sample to have either a small crystal sizes or a disordered structure.

FTIR spectra.

As it was described in the preparation method, Li-VPO-u was prepared intending to intercalate the Li cations between the layers of the $VOPO_4*2H_2O$. To determine that Li^+ intercalation took place, the OH group vibration frequencies in the IR spectra were followed since any alteration of the interlayer water of the $VOPO_4*2H_2O$ caused by intercalation, should be reflected in either the position or in the shape of the IR absorption peaks.

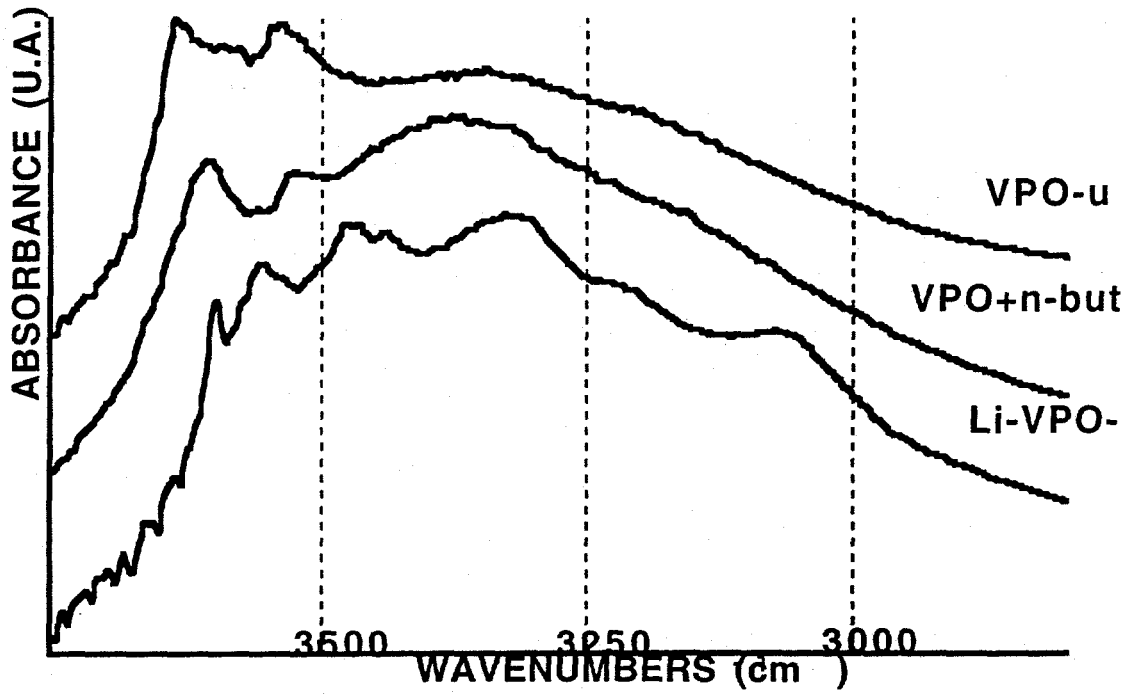

Figure 4a . FTIR spectra for several samples in the regions (3750-2900 cm^{-1})

In figures 4a and 4b, the FTIR spectra at (3750-2900 cm^{-1}) (4a) and (1750-1550 cm^{-1}) (4b) for VPO-u and Li-VPO-u are presented. The OH stretching (ca. 3300 cm-1) and OH bending (ca. 1650 cm-1) vibration modes appear in these regions of the IR spectra. According

to the literature (17), the narrower features in the stretching zone of $VOPO_4*2H_2O$ (VPO-u) have been assigned to the strongly bounded water molecules coordinated to V atoms, and the broader band, to the loose water molecules held between the layers by hydrogen bonds with the PO_4 groups. In the bending zone, the OH vibration modes arising from both kind of water molecules are overlapping. The Li-VPO-u spectra in both of these wavenumber regions show a completely different IR pattern. New bands which are not present in the VPO-u spectrum appear in the Li-VPO-u one. It is clear that after intercalation, water molecules are affected by

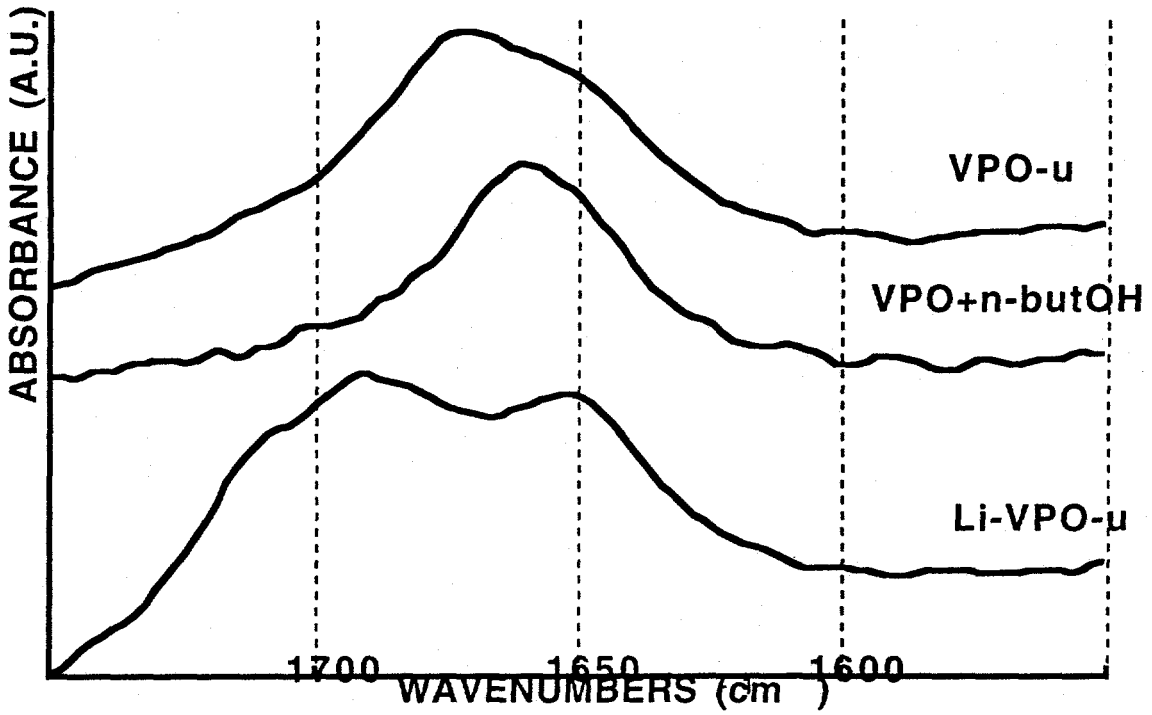

Figure 4-b: FTIR spectra for several samples in the regions (1750-1550 cm^{-1}).

interactions occurring in the interlayer space resulting in new vibrational frequencies. These new features in the Li-VPO-u samples can not be due to the intercalation of n-butanol used to wash the precipitate, since a VPO-u sample treated with n-butanol solution overnight at 323 K exhibits a spectrum referred as "VPO+n-butOH" which is quite similar to the VPO spectrum. It is likely that in the Li-VPO-u sample, the intercalated Li cations interacts with the water molecules changing their vibration modes which accounts for the new features observed in this catalyst. Therefore the IR evidence indicates that intercalation of Li^+ was attained in the Li-VPO-u sample. In figure 5, the 1500-500 cm^{-1} region of the spectra for some of the unsupported calcined and uncalcined samples are presented. Table 1 summarizes the observed bands along with the proposed assignments to vibration modes according to the results reported in the bibliography (35-37).

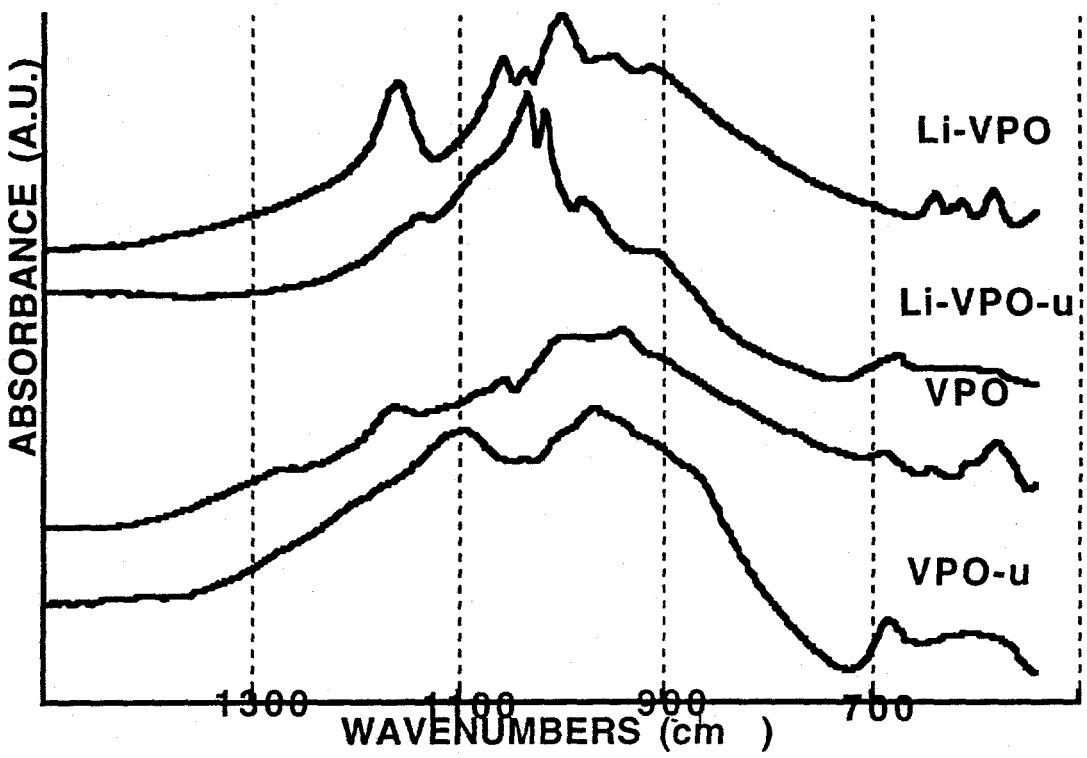

Figure 5: FTIR spectra for several samples in the region (1750-1550 cm^{-1}).

The VPO-u spectrum is very similar to the spectra of the $VOPO_4*2H_2O$ (17, 35, 38). The spectrum of the calcined VPO, however, shows vibrations at 1093 (s), 1045 (w) and 968 (s) cm^{-1} shifted to 1163 (s), 1055 (m) and 941 (s) cm^{-1} and the (P-O) bending vibration zone shows four different bands. An irreversible phase change from a_I-$VOPO_4$ to a_{II}-$VOPO_4$ has been reported to take place at 993 K (9). These two phases are very similar and there are only small differences in the relative positions of the V and P atoms in the structure (18, 19). It is likely that either the VPO-u sample has undergone the phase change at lower temperature than reported, or that the spectra of the VPO sample showed in figure 4 represents a state in which a partial phase change has occurred. In any case, whichever the final structure is, the resulting phase is going to have a layered $VOPO_4$ structure.

The Li-VPO-u spectrum is completely different to the VPO-u one. The most evident alteration is the splitting of the n(V=O) at 1000 cm^{-1} (sh) band into two new bands at 1014 (s) and 980 (m) cm^{-1} in the Li-VPO-u spectrum. In addition, in the VPO-u spectrum the bands at 1093 (s), 1045 (w), 874 (sh) cm^{-1} bands shifted to 1138 (w), 1032 (s) and 914 (m) cm^{-1} in Li-VPO-u spectrum. The changes in the n(P-O) modes can be due to an alteration of the vibration modes of the P-O bonds caused by Li^+ intercalation. On the other hand it has been reported that

the n(V=O) frequency is strongly influenced by the vanadium valence state: the n(V^{V}=O) is placed at around (1000-1030) cm^{-1} and n(V^{IV}=O) around (980-1000) cm^{-1} (17, 35). The two bands at 980 and 1014 cm^{-1} can represent two different vanadium valence state which arise from the redox intercalation process. Therefore, all the changes in the IR frequencies of the Li-VPO spectrum can be ascribed to Li^{+} intercalation. This alterations in the frequencies of the vibration modes is another evidence that Li^{+} intercalation between the $VOPO_4$ layers took place.

Table 1. Assignments of the FTIR bands to vibration modes in the region (500-1500 cm^{-1}) for some of the unsupported samples.

VPO-u	VPO	Li-VPO-u	Li-VPO	Assignment
1093 (s) 1045 (w)	1163 (m) 1055 (m)	1138 (m) 1032 (s)	1157 (s) 1055 (s) 1034(m)	u_{as}(P-O)
1000 (sh)	1000 (s)	1014 (s) 980 (m)	1000 (s)	u(V=O)
968 (s) 874 (sh)	941 (s) 900(w)	968 (sh) 914 (m)	949 (m) 912 (m)	u_{s}(P-O)
683 (m) 608 (m)	687 (m) 642 (m) 608 (m) 579 (m)	675 (m)	700 (w) 636 (m) 611 (m) 580 (m)	d_{s}(P-O)

The calcined Li-VPO sample displays a spectra with features with frequencies close to the values of the calcined VPO; but the peaks are more resolved and sharper. This indicates that the Li-VPO structure is similar to the VPO one but with more regular V-O and P-O bonds. In addition the n(V=O) mode is located at 1000 cm^{-1} which means that V valence state is 5 (this sample has been calcined in air at 873 K). It does not seem possible that the Li cations are still between the layers. Firstly because there are no major changes in the vibration modes frequencies of the calcined VPO with Li-VPO samples. Secondly because after calcination there is no V^{IV} stabilizing the Li^{+} cations between the layers. As a result the Li cations during calcination are likely to migrate to the surface and remain highly interdispersed onto the VPO phase.

XPS results.

The binding energy for the $V2p_{3/2}$ peak was centered around 517 eV and Li1s was detected at 54.7 eV, which agrees with the reported binding energy for V^{V} (39) and Li^{I} (40).

The XPS intensity ratio I_{Li}/I_V for the Li1s and the $V2p_{3/2}$ peaks in the unsupported catalysts are summarized in Table 2. The results indicate that the I_{Li}/I_V ratio for the Li-VPO is bigger than the Li-VPO-u one, which means than the surface of the calcined sample is richer in Li than the precursor. As it was already stated, the Li-VPO-u sample may be described as $VOPO_4*nH_2O$ intercalated with Li^+. During the intercalation process the V^V of the structure is reduced to V^{IV}, which allows the Li^+ to be placed between the $VOPO_4$ layers. When the sample is calcined, the V^{IV} may be oxidized, making the Li interlayer unstable and the Li cations may migrate to the surface of the solid, which explains the Li^+ enrichment on the calcined Li- VPO.

The I_{Li}/I_V ratio for the samples prepared by coprecipitation is bigger than for the Li-VPO systems (16 times for precursor and 6 times for calcined samples). Therefore the surface of the *coprecipitated* uncalcined Li-VPO is richer in Li than Li-VPO. On the other hand, no enrichment in Li is observed when the coprecipitated precursor is calcined. It seems likely that the last phase which precipitates during the preparation procedure is richer in Li and this would explain why the surface of *coprecipitated* Li-VPO-u is more concentrated in Li. Moreover, in this preparation method V^V is not reduced to V^{IV}, and the Li^+ can not be stabilized in the structure of the VPO phase. Hence, when the coprecipitated Li-VPO-u sample is calcined no Li^+ migration from the bulk occurs, and this is the reason of the similar value obtained in this system after calcination.

Table 2. XPS intensity ratio I_{Li}/I_V for the Li1s and $V2p_{3/2}$ peaks in the unsupported catalysts.

SAMPLE	**I_{Li}/I_V ratio** (A.U.)
Li-VPO-u	3.4
Li-VPO	8.1
coprec. Li-VPO-u	54.2
coprec. Li-VPO	49.5

Table 3. Percentage of the different O_2 isotopes in the outlet (referred to the total oxygen present in the flow) after 4 min of $^{18}O_2$ exchange on various supported catalysts at 923 K.

	Gas phase reaction	VPO/SiO2	Li-VPO/SiO2	SiO2	Li/SiO2
% $^{16}O_2$	2.88	9.68	19.72	23.42	45.43
% $^{16}O^{18}O$	6.31	6.62	10.77	6.59	4.01
% $^{18}O_2$	90.81	83.7	69.51	69.99	50.56

CATALYTIC RESULTS.

Figure 6 shows the % of CH_4 conversion as a function of the temperature for the unsupported VPO and the Li-VPO catalysts. One of the most interesting result of this work is that the *coprecipitated* Li-VPO catalyst *was not active* in the 600-700°C temperature range, hence only results for the *intercalated* Li-VPO catalyst are presented. Li-VPO, although almost twice more selective to FA, is slightly less active than VPO. The reaction products were CO, CO_2, HCHO and H_2O with no C_2 hydrocarbons detected.

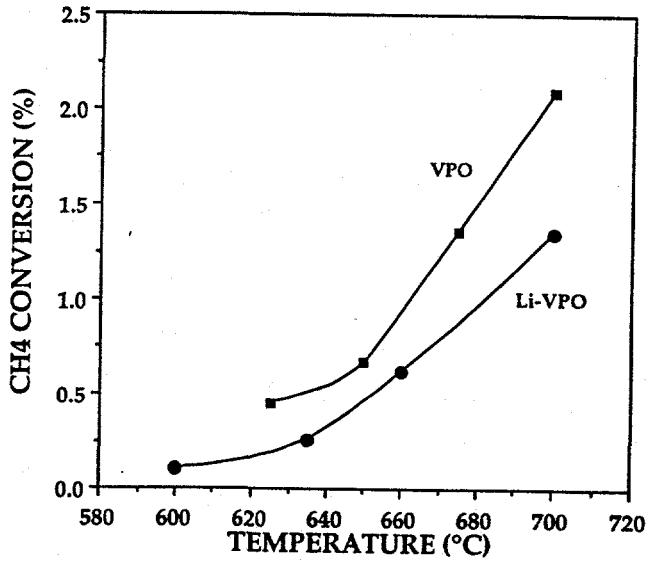

Figure 6. Methane conversion as a function of temperature for VPO and Li-VPO unsupported catalysts.

The FA selectivity vs. methane conversion for the unsupported catalysts is shown in fig. 7. As in the case of many consecutive partial oxidation reactions, the selectivity to the intermediate, FA, decreases as conversion increases

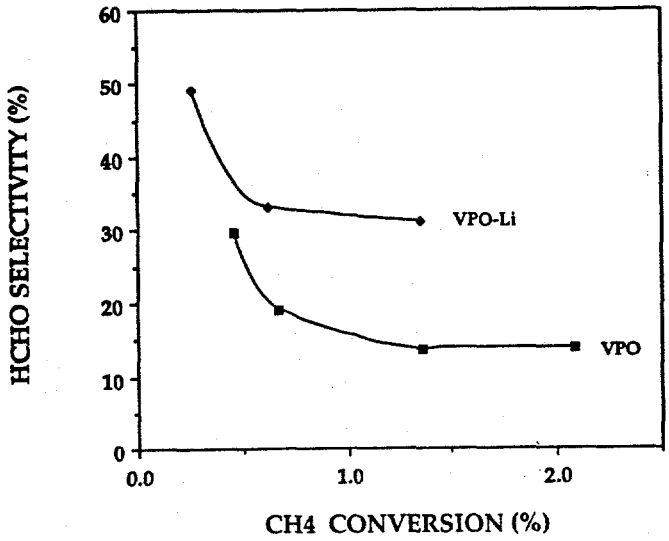

Figure 7: HCHO selectiviyt as a function of methane conversion for the VPO and LiVPO catalysts.

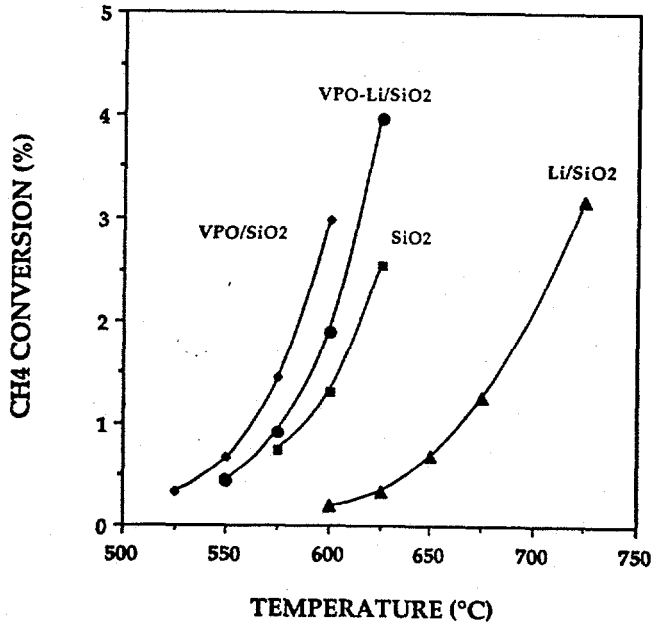

Figure 8: CH_4 conversion (%) as a function of temperature for several supported catalysts (conditions as indicated in experimental section).

The catalytic activity for the supported catalysts and SiO_2 are shown in figure 8 in terms of CH_4 conversion as a function of temperature. The conversions for the supported catalysts were higher (up to 4%) than on the unsupported catalysts results, as expected from their higher surface areas. SiO_2 shows some activity but it is lower than the supported VPO catalysts, and the Li-VPO/SiO_2 sample is slightly less active than VPO/SiO_2. On the other hand Li supported on silica prepared with the same procedure used to add the Li^+ to the VPO/SiO_2 precursor has the lowest catalytic activity of the catalysts shown in this figure and requires about 100°C higher temperature to yield an equivalent conversion.

The FA selectivity as a function of CH_4 conversions is presented in figure 9 for the supported catalysts. As in the case of the unsupported samples, the lithiated sample is much more selective than the unpromoted one for both the SiO_2 and VPO/SiO_2 samples. In addition, SiO_2 shows as much FA selectivity as VPO/SiO_2 but occurring in a higher temperature range. It has been reported that SiO_2 is able to selectively oxidize methane to FA, thus the selectivity depends on the kind of SiO_2 used (41-43). Therefore, the SiO_2 itself is able to activate methane and form the appropriate intermediates which yield FA. However, it is unlikely that the support is the major responsible of the CH_4 activation in the case of the SiO_2 supported VPO catalysts because the later catalysts are active in a lower temperature range in which SiO_2 is not active (see figure 6). It must be also noted than the Li/SiO_2 sample is very selective, as much as the Li-VPO/SiO_2 sample which shows that some Li^+ species present in the Li/SiO_2 surface are able to oxidize methane selectively.

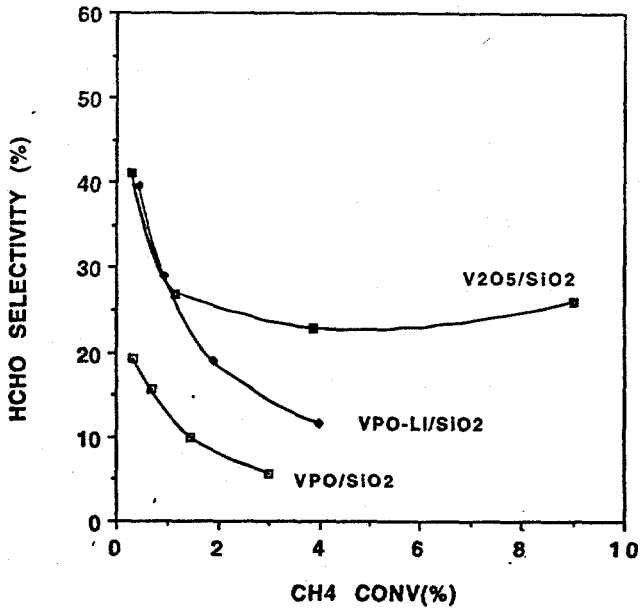

Figure 9: HCHO selectivity(%) as a function of CH_4 conversion (%) for the same catalysts of fig. 8.

Double bed experiments. In figure 10 the FA selectivity vs CH_4 conversion of the double bed configuration (VPO/SiO_2 + Li/SiO_2) are compared with the single bed experiments (VPO/SiO_2) at two different GSHVs. The single bed runs were done under similar experimental conditions than on the double bed runs, but placing only VPO/SiO_2 in the reactor.

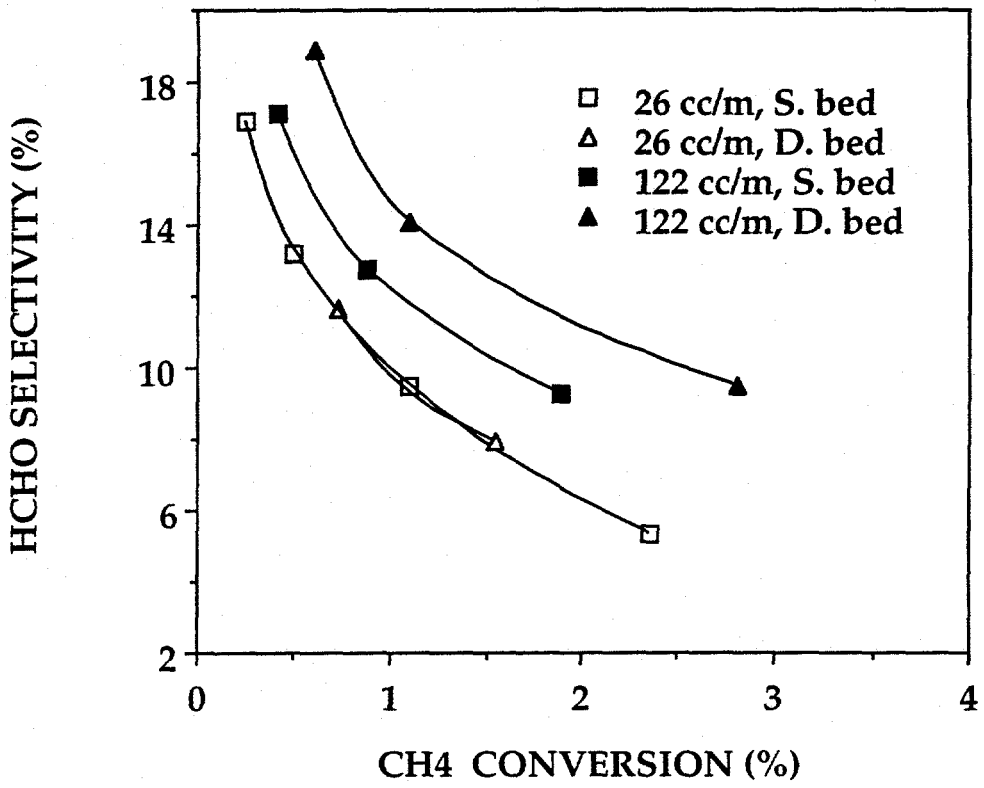

Figure 10: Comparison of the HCHO selectivity vs CH_4 conversion curves in double bed and single bed configurations at two different flow rates (conditions as indicated in experimental section).

At low space velocity, there is no difference in the catalytic behavior of the double and single bed configuration. However, when the flow rate is increased, the double bed configuration shows higher selectivity than the single bed arrangement. It is important to emphasize again that, as it can be seen in figure 8, the Li/SiO_2 sample shows a very small activity in the temperature used in these experiments (848 K). Therefore the contribution of the Li/SiO_2 sites present in the Li-VPO/SiO_2 catalysts to the total activity is very small. It must be taken into account that the amount of Li/SiO_2 used in the double bed experiment is even smaller than in the results showed in figure 8. In the case of the run at higher GHSV, this contribution must be even much smaller since the contact time is lower. The selectivity conversion curves at

the faster flow rate are higher than at the low flow rate. This is apparently the result of the lower contact time of the FA intermediate with the oxidizing surfaces.

TRANSIENT EXPERIMENTS

Figure 11 shows the concentrations for the different O_2 isotopes after a step increase in $^{18}O_2$ concentration was introduced in the reactor containing the supported Li-VPO/SiO_2 catalyst. After the introduction of the $^{18}O_2$ step (after a delay of about 70 s. due to dead volume) the mass spectrometer detected $^{18}O_2$, $^{18}O^{16}O$ and $^{16}O_2$ in the effluent. The $^{16}O_2$ arises from the exchange of gas phase $^{18}O_2$ with the lattice oxygen. The $^{18}O^{16}O$ is due to the scramble between the $^{18}O_2$ and the $^{16}O_2$. The other catalysts studied presented a similar behavior to the one showed in figure 11: a sudden increase of the $^{16}O_2$ concentration due to the exchange between the gas phase $^{18}O_2$ and the ^{16}O atoms of the lattice, which decreased smoothly after reaching a maximum short time after the step was introduced.

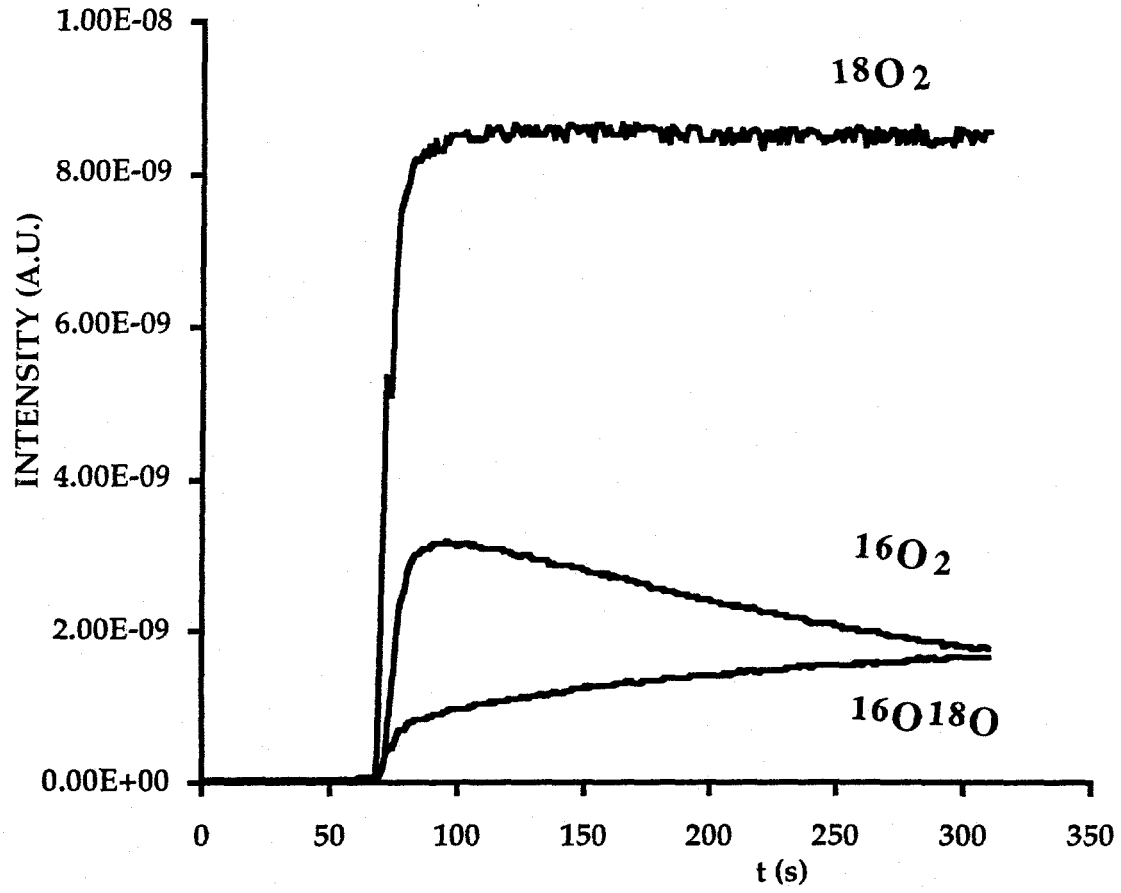

Figure 11. $^{18}O_2$, $^{16}O_2$ and $^{16}O^{18}O$ concentrations in the effluent when a $^{18}O_2$ step in He is fed through a Li-VPO/SiO2 at 923 K.

The extent of exchange depends strongly of the type of catalyst used, and different amount of isotopic exchange is obtained for the different samples. Table 3 summarizes the percentage of each O_2 isotope with respect to the total O_2 in the outlet after 4 minutes of analysis. The column "gas phase reaction" refers to the response in an unloaded blank reactor and in this case the $^{16}O_2$ and scrambled oxygen detected are due to these species present as impurities present in the $^{18}O_2$ feed. Table 3 shows that each catalyst exhibits different % of oxygen exchange capabilities. The VPO/SiO_2 catalyst exhibits the lowest percentage of exchange which means that this catalyst has the slowest gas phase-lattice oxygen exchange rate. On the other hand, Li/SiO_2 exhibits the fastest exchange rate whereas $Li\text{-}VPO/SiO_2$ shows an intermediate exchange behavior between these two samples. SiO_2 itself exhibits similar exchange rate than the $Li\text{-}VPO/SiO_2$ catalysts. It must be stressed that Li/SiO_2 shows a much higher oxygen exchange rate than $Li\text{-}VPO/SiO_2$, even if the amount of Li is the same in both samples. This indicates that the Li in the VPO phase is quite different than in the SiO_2 support.

While the conversion and selectivity obtained with the Li-VPO catalyst are similar to those previously reported, the different results obtained depending on the method of introduction of the Li promoter can be significant in the design of more active and selective catalysts. The catalytic results reported here clearly show that the Li cation improves the FA selectivity on VPO phases. It is also evident that the method used to add the Li^+ strongly influences the catalytic behavior. In order to obtain an active and selective catalyst, Li^+ has to be intercalated between the layers of the $VOPO_4*2H_2O$ which upon calcination forms the active phase.

The role of Li^+ and VPO phase in these catalysts and why the intercalation is the more effective method to add the Li^+, can be explained on the basis of the characterization results. The VPO-u sample is $VOPO_4*2H_2O$ as it was deduced from the XRD and FTIR results. When this sample was calcined, a disordered phase (according to XRD data) was formed (VPO); which is very likely either $a_I\text{-}VOPO_4$ or $a_{II}\text{-}VOPO_4$ or some intermediate state between the a_I and a_{II} phases. A similar situation is expected in the unpromoted *supported* catalyst and a low dispersion is expected because of the weak interaction between this phase and SiO_2 (44). The structure of the Li *coprecipitated* catalyst is unknown, but the XPS results allowed to deduce that its surface is the richest in Li^+ among all the Li promoted samples studied. It can be assumed that a Li^+ phase is covering most of the surface of the *coprecipitated* catalyst. The unsupported Li intercalated precursor (Li-VPO-u) can be considered to be $VOPO_4*2H_2O$ with a disordered crystalline structure because of the intercalation of Li^+ between the $VOPO_4$ layers. When this sample is calcined, its FTIR spectrum is similar to the VPO one. It follows that both catalysts have a similar structure and therefore the intercalated Li^+ was removed off the interlayer space as a consequence of the calcination and migrated to the surface of the grains (XPS results). The surface concentration of Li^+ in the Li-VPO however is smaller than for the *coprecipitated* catalyst (around 6 times smaller) indicating that there is less Li^+ covering the

surface of the calcined Li-VPO catalyst. The existence of a $M_2VO_2PO_4$ phase ($M=Sr^{2+}$, Ba^{2+} y Ag^{+}) has been reported (45, 46). The vanadium is as V^V and the M^{n+} cations are placed between the layers defined by VO_6 octahedra couples and PO_4 tetrahedra. Li^+ is a much smaller cation than Ag^+ and consequently could also be embedded in the "VO_2PO_4" structure. The formation of a $Li_2VO_2PO_4$ structure in the surface would withdraw Li^+ from the interlaminar space of the $VOPO_4$ structure, and a core of $VOPO_4$ phase would be formed in the kernel of the catalyst grain which is the phase detected by FTIR. It must be noticed that the I_{Li}/I_V in the Li-VPO sample is around twice the value for uncalcined sample (Li-VPO-u) which may be due to the fact that a $Li_2VO_2PO_4$ phase is formed in the outmost layers of the Li-VPO catalyst. The formation of such a phase in the outer layers of the catalyst grain would allow an atomic dispersion of the Li cations on a VPO phase without the formation of a seggregated Li phase covering the VPO phase. Although the existence of $Li_2VO_2PO_4$ can not be asserted with certainty because the FTIR of the $Li_2VO_2PO_4$ is unknown, it can be suggested that after calcination the Li cations are dispersed and embedded in a VPO phase. In the SiO_2 supported catalyst, the Li^+ intercalation should result in similar phases as in the unsupported ones since $VOPO_4*2H_2O$ is expected to be deposited on the SiO_2. In addition, a Li/SiO_2 phase can also be formed but it was shown that it is less active than the VPO containing catalysts.

The fact that on Li-VPO/SiO_2 the oxygen isotopic exchange rate was different than on the Li/SiO_2 catalyst indicates that the Li^+ species in the promoted supported catalyst are different to the ones present in the Li/SiO_2 catalyst. The most likely Li phase in the Li/SiO_2 catalyst is a lithium oxide which can be well dispersed but it is not combined with another phase. The difference in the isotopic exchange indicates that the lithium oxide phase is not present as a major component in the Li-VPO/SiO_2 catalyst. Instead the Li phase dispersed, embedded in and related with a VPO phase can explain the difference in the oxygen exchange rate. Since it can be expected that the supported phase present in the Li-VPO/SiO_2 catalyst is the same that in the unsupported Li-VPO catalysts, it can be assumed that the same Li dispersed phase is responsible for the selectivity of the unsupported catalyst.

While dispersed Li contributes to the selectivity of the promoted sample, it is clear that the VPO phase itself is able to activate CH_4 since the unsupported VPO is active. In silica supported catalysts, SiO_2 could activate CH_4 since SiO_2 itself shows some catalytic activity at high temperature (figure 7). However, CH_4 conversion must be occurring mainly on the VPO phase since it exhibited conversion at temperatures where SiO_2 alone was not active. The most probable pathway for CH_4 activation on a VPO surface could be via interaction of CH_4 with O^- or O_2^-, as it has been proposed for other metal oxides (47, 48). A possible explanation for the low FA selectivity on VPO phases when compared with metal oxides reported in the bibliography could be the existence of the M-O-M bridges which exist in the crystalline structure of the $VOPO_4$ system and which have been claimed as non selective centers in the case of MoO_3 system (7, 49, 50). On the other hand, the Li^+ species present in the various Li

doped catalysts do not seem the main pathway for CH_4 activation. Li/SiO_2 is the least active catalyst and the Li-VPO, whose surface is Li^+ enriched shows lower activity than VPO. In addition, the coprecipitated catalyst whose surface is the richest in Li^+ and that could be described as covered by a Li^+ phase, was not active at all.

Li^+ species themselves are very selective as it is deduced from the fact that the Li/SiO_2 catalyst is one of the most selective reported in this work. The double bed experiments show that some intermediates created on the VPO phase (first catalytic bed) can reach the Li^+ species placed downstream if a fast enough space velocity is used. This Li^+ species further oxidize selectively the intermediates. These two facts suggest that the Li^+ species in the promoted VPO catalysts can oxidize selectively the intermediates created during CH_4 activation on the VPO centers. Another explanation that can also be proposed assumes that the Li-VPO centers present on the surface of the promoted catalyst may have higher FA selectivity than VPO centers. This assumption can not be discarded, even if the previous suggestion seems to be more likely.

The nature of the intermediates created in the CH_4 activation can not be ascertained with the experimental data obtained in this work. However, it is not likely that methyl radicals form on the unpromoted VPO surface, as it has been proposed for other catalysts (47, 51). Otherwise, some C_2 hydrocarbons could have been detected in the double bed experiments performed at higher space velocity since some CH_3 radicals could recombine in the gas phase instead of being transformed by the Li phase to FA.

Li doped catalysts are well known methane coupling oxidation catalysts (52-56) and Li^+ species have been always related to the oxidative dimerization: Li^+ species have not been claimed as sites able of selectively oxidizing methane. In Li/MO systems it has been suggested that $[Li^+O^-]$ centers generated from the substitution of the M^{2+} cation by Li^+ in the metal oxide lattice (50-53) or F-type centers formed from $[Li^+O^-]$ (56) can be the active centers. This substitution is only possible if the M^{2+} radius is quite similar to the Li^+ radius and if the system is at high temperatures (>823 K). Methane has been proposed to react with these centers, which abstract a H radical from the CH_4 and form CH_3 radicals. The CH_3 radicals react further in the gas phase to form the higher hydrocarbons. The possibility that such $[Li^+O]$ centers are formed in the Li promoted VPO catalysts can not be discarded since the V^V cation have similar size than Li^+ (Li^+=68 ppm and V^{5+}=59 ppm) (57). Nevertheless, if some C_2 hydrocarbons are formed in the gas phase reaction is very likely that they will be burned by the VPO phase to carbon oxides. On the other hand, it is not surprising that in the Li/MO systems investigated up to now no FA has been reported since much higher temperatures were used (>973 K). In fact in the Li/SiO_2 catalyst significant amounts of C_2 hydrocarbons were formed when the temperature was higher than 973 K. In the Li doped VPO samples reported here, the capability of the VPO phase of activating the CH_4 and forming the appropriate intermediates at relatively lower temperatures, makes it possible that such intermediates could further evolve and form FA.

The extent of exchange depends strongly of the type of catalyst used, and different amount of isotopic exchange is obtained for the different samples. Table 3 summarizes the percentage of each O_2 isotope with respect to the total O_2 in the outlet after 4 minutes of analysis. The column "gas phase reaction" refers to the response in an unloaded blank reactor and in this case the $^{16}O_2$ and scrambled oxygen detected are due to these species present as impurities present in the $^{18}O_2$ feed. Table 3 shows that each catalyst exhibits different % of oxygen exchange capabilities. The VPO/SiO_2 catalyst exhibits the lowest percentage of exchange which means that this catalyst has the slowest gas phase-lattice oxygen exchange rate. On the other hand, Li/SiO_2 exhibits the fastest exchange rate whereas $Li\text{-}VPO/SiO_2$ shows an intermediate exchange behavior between these two samples. SiO_2 itself exhibits similar exchange rate than the $Li\text{-}VPO/SiO_2$ catalysts. It must be stressed that Li/SiO_2 shows a much higher oxygen exchange rate than $Li\text{-}VPO/SiO_2$, even if the amount of Li is the same in both samples. This indicates that the Li in the VPO phase is quite different than in the SiO_2 support.

SUMMARY OF SECTION 7-1.

The conversion and selectivity obtained with the Li-VPO catalyst are similar to those previously reported for other catalysts. The results depended on the method of introduction of the Li promoter. The catalytic results clearly show that the Li cation improves the FA selectivity on VPO phases. It is also evident that the method used to add the Li^+ strongly influences the catalytic behavior. In order to obtain an active and selective catalyst, Li^+ has to be intercalated between the layers of the $VOPO_4*2H_2O$ which upon calcination forms the active phase. While the results regarding the role of Li could be significant in designing other catalysts for this reaction, the Li/VPO catalyst exhibited the type of low selectivity at low conversion characteristic of other catalyst reported in the literature. For this reason no further studies of this reaction pathway was conducted, and attention was focused on the oxidative coupling reaction.

7-2 TRANSIENT STUDIES OF METHANE OXIDATIVE COUPLING ON $Li/LaNiO_3$ CATALYSTS.

Initial experiments, presented in section 7-3, with metallo oxides of Co. Ni and Rh showed that their C_2 selectivity was low without Li promoter. Furthermore only the Li promoted $LaNiO_3$ catalyst exhibited selectivities that warranted further studies. This section focus on the use of transient techniques to study the role of Li promotion exclusively on the $Li/LaNiO_3$ catalyst. Further studies with the other metallo oxide catalyst are presented in section 7-3 in the context of the partial oxidation to syngas.

CATALYST PREPARATION

$LaNiO_3$, $LaCoO_3$ and $LaRhO_3$ oxide were prepared by combining stoichiometric amounts of nitrates of Ni, Co and Rh and $La(NO_3)_3$ into de-ionized water. After dissolving the nitrates, citric acid was added to the mixture in such amount that the molar ratio of the sum of

the nitrates to that of citric acid was equal 1. After evaporating the water the remaining powder was heated to 450°C and later calcined at 700°C in oxygen flow for two hours.

Lithium promoted $LaNiO_3$ catalysts were prepared by the same method described above, however a small amount of lithium carbonate corresponding to a particular weight percentage of Li was added to the solution of Ni and La nitrates. Prior to each experiment, all catalyst samples were pretreated in an oxygen flow for 2 hours at 700°C.

CATALYSTS CHARACTERIZATION.

X-ray diffraction.

Results of the X-ray diffraction experiments for unpromoted and 1% Li promoted catalyst are presented in Fig. 12. XRD patterns indicate that there are significant changes in the major XRD lines of $LaNiO_3$ with the addition of small amount of Li. While the unpromoted catalyst has XRD lines characteristic only for the perovskite structure of $LaNiO_3$, the Li promoted catalyst exhibits additional lines characteristic for Li_2CO_3. This behavior indicates that the presence of lithium plays rather significant role during preparation of the Li promoted catalyst. When sodium was used as an alkaline dopant in $LaNiO_3$ (results not shown), no changes in the XRD structure were observed. Hence, it can be concluded that in the case of lanthanum nickel oxide the presence of lithium but not sodium can modify the final composition of the catalyst.

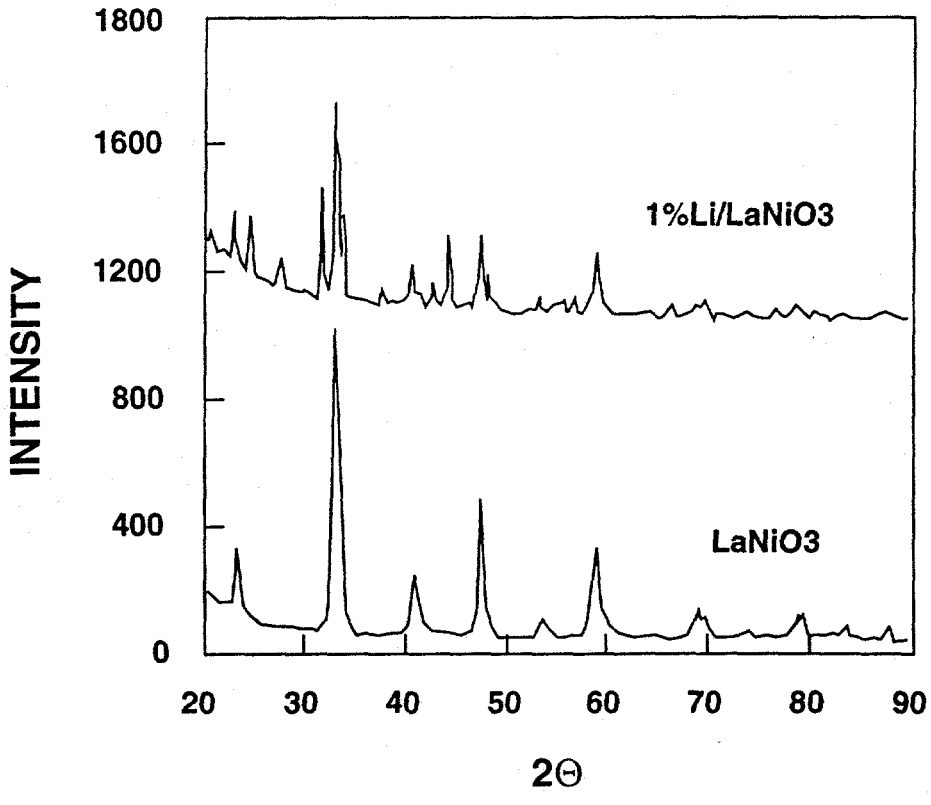

Figure 12. XRD patterns of unpromoted and Li promoted $LaNiO_3$.

BET surface areas

The surface area for the $LaNiO_3$ phase was found to be around 4.2 m^2/g, and after lithium promotion, the total surface area decreased to 2.9 m^2/g for the 1% Li promoted $LaNiO_3$. Measurements were taken on fresh samples at room temperature and prior to each experiment, the catalyst was degassed for 2 hours in a helium flow at 120°C. The decrease in the surface area after Li promotion is a typical behavior observed for the majority of oxidative coupling catalysts. This can be explained by the formation of surface species such as Li carbonates and mixed oxides which block the pores of the precursor. Due to this behavior it is also likely that the addition of Li will change the nature of the interaction between CH_4 and the surface of the catalyst during oxidative coupling reaction.

ACTIVITY AND SELECTIVITY MEASUREMENTS.

In the presence of the unpromoted $LaNiO_3$ catalyst CH_4 and O_2 start to react at about 450°C, and complete oxygen conversion is achieved around 550°C. These temperatures are much lower than those usually encountered in oxidative coupling indicating a significant

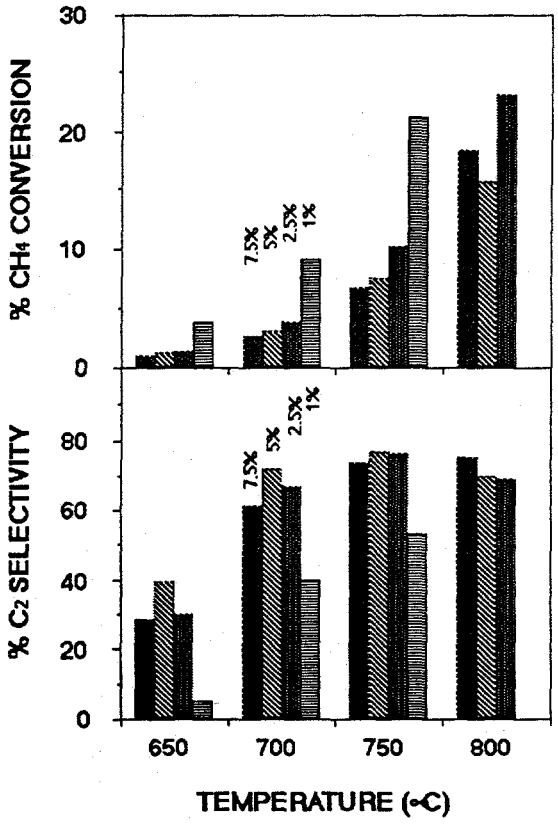

Figure 13. CH_4 conversion and C_2 selectivities vs reaction temperature during OC reaction at different Li loadings.

interaction of methane with the catalyst surface. This interaction however, is too strong since it leads to a complete oxidation of methane to yield CO_2. The effect of lithium loading on

conversion, and product selectivity as a function of reaction temperature is presented in figure 13. Addition of Li suppresses significantly the high activity for total oxidation displayed by the unpromoted catalysts and shifts the reaction temperature to a range typical for the methane oxidative coupling. At a given temperature as lithium loading increases, the conversion decreases except at 800°C. These results indicate that Li promotion eliminates some of the sites for significant methane-surface interaction present in the unpromoted catalyst, and shifts the

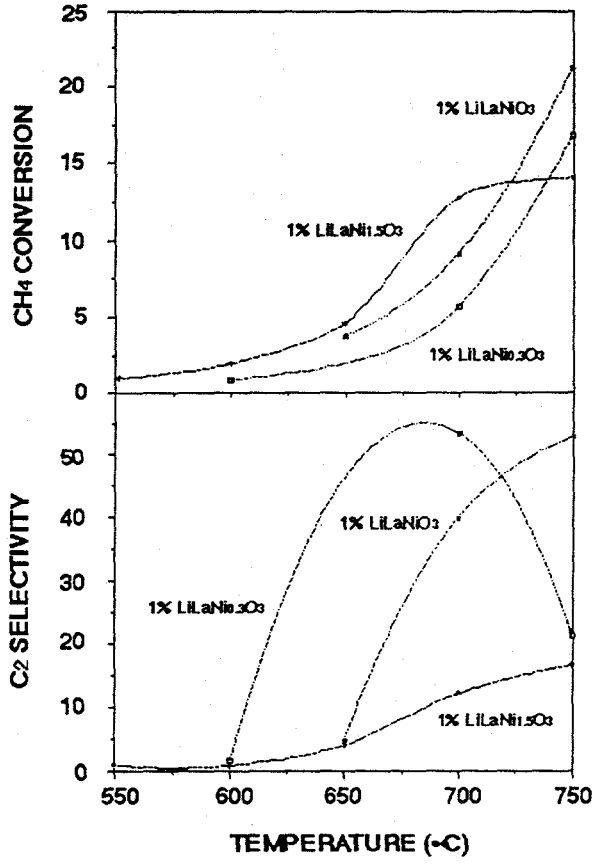

Figure 14. Conversion of CH_4 and C_2 selectivity on $LaNiO_3$ catalyst with different Ni/La ratio.

reaction to the free radical mechanism which predominates at high temperature (58).The bottom half of Figure 13 shows the effect of Li loading on C_2 selectivity. In this case, except for the 1% loading, the selectivity is about the same in each case and increases with temperature levelling off at around 70% in the temperature range of 700-800°C. The catalyst promoted with 1% Li has a slightly slower selectivity but exhibits the highest conversion, hence it has the highest yield and it was selected for further study. These results indicate that the suppression of activity coincides with the elimination of the combustion sites which allow for the formation of the free radicals which recombine in the gas phase to form C_2 hydrocarbons. Previous work on methane steam reforming has shown that methane interaction with a nickel based catalyst

(nickel aluminates) was affected by the ratio between the metal oxide and the alkaline oxide (59). Figure 14 shows the conversion-selectivity results as a function of temperature for two other catalysts with excess and deficiency of Ni in relation to the La oxide. The stoichiometric material exhibits the highest yield whereas the selectivity of the nickel deficient catalyst goes through a maximum and it is rather low for the catalyst with excess Ni. The latter material yields mainly CO_2. Thus, the presence of Li modifies sites associated with surface Ni since when they exceed the Li loading such sites are still capable of complete combustion of methane or the C_2 products. Time on stream experiments with the 1% Li loading catalysts reveal that during a five hour period, conversion remains fairly constant, but selectivity decreases with time. This decrease is likely due to the loss of Li leading to the exposure of the combustion sites present in the unpromoted catalysts. To further understand the role of Li promotion a series of transient experiments was conducted.

TRANSIENT STUDIES.

Pulses of pure methane diluted in helium with no oxygen were passed over 20 mg of the unpromoted $LaNiO_3$ at 700°C. The results presented fig. 15, show the appearance of a mass

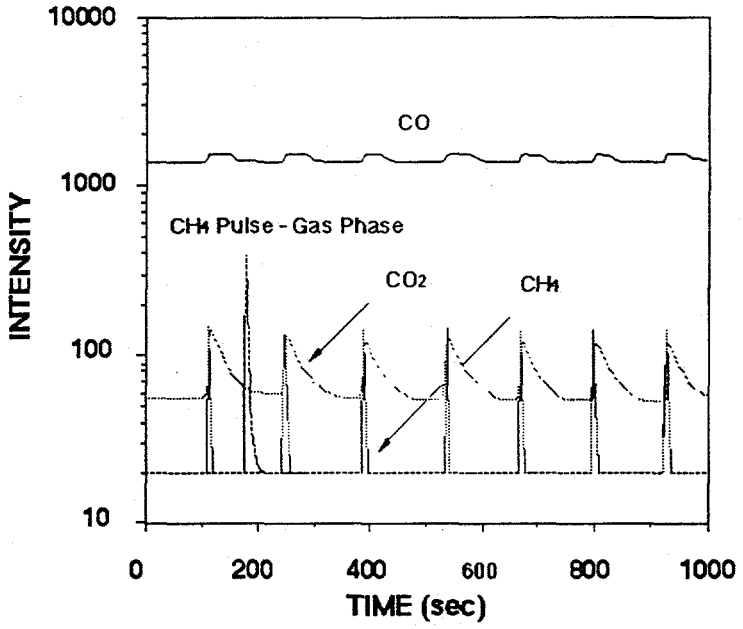

Figure 15. Pulses of methane over $LaNiO_3$ catalyst at 700°C. Mass of the catalyst 20 mg.

signal corresponding to CO_2 and no C_2 signal. The CO_2 signal has a significant tail indicating a strong interaction of CO_2. Also displayed is the signal obtained in the absence of the catalyst showing no CO_2 formation in the gas phase. These results indicate that either there is a participation of lattice oxygen in the formation of CO_2 since no oxygen was present in the pulses, or that some reduction of the nickel oxide is taking place. Results of pulses of methane

containing 12, 9, 6 and 3% oxygen (vol), passed over the unpromoted Li catalyst at 550°C are shown in figure 16. The reaction temperature was lowered due to the higher reactivity of $LaNiO_3$ found in the presence of oxygen. As in the previous case with pure methane, only CO_2 is observed as a reaction product with no traces of C_2 formation and only a minor trace of CO. In both cases with and without oxygen, the only product detected is CO_2 showing that fast combustion of methane or the C_2 products is occurring on the combustion sites.

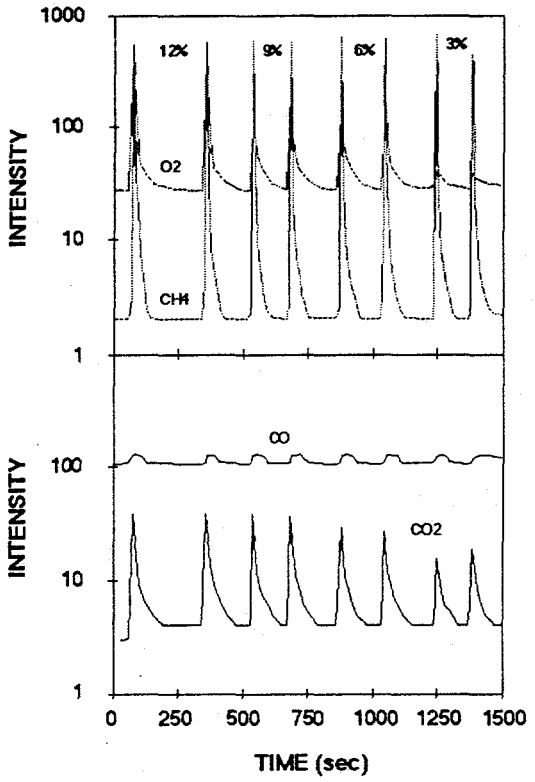

Figure 16. CH_4 pulses with different O_2 concentration on $LaNiO_3$ at 550°C.

Similar experiments consisting of pulses of methane containing oxygen at various oxygen concentration over a 2.5% $Li/LaNiO_3$ at 700°C show that there is no C_2 product evolving in this case, in fact not even CO_2 is detected (fig. 17). This rather interesting finding indicates that whatever product is formed during pulses over Li promoted catalyst, it is captured on the surface of the catalyst. Since the catalyst used in this experiment has been exposed to reactants, the experiments were repeated at lower temperatures but on a fresh samples and on a CO_2 treated catalyst. The results, shown in figure 18, indicate that indeed some CO_2 formation is observed in the presence of the fresh catalyst, but the signal decreases with the number of pulses used. In the case of the CO_2 treated catalyst (1 hr at 500°C), no

measurable CO_2 signal appears in agreement with the experiments presented in fig. 16 for an aged catalysts. These results show that during transient experiments some surface compound is

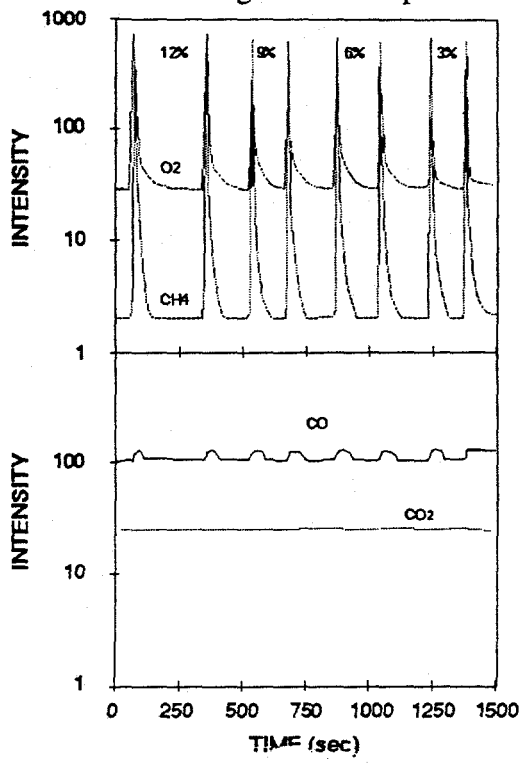

Figure 17. CH_4 pulses with different O_2 concentration on 2.5% $Li/LaNiO_3$ at 700°C.

formed from the reaction products and becomes trapped on the surface. The most likely product formed is CO_2 which presumably can form a surface carbonates. For the fresh catalysts, the results indicate that such reaction is initially less significant but it becomes more important as time on stream (or number of pulses) increases. If the surface intermediates were carbonates it would imply that they are involved in the formation of CO_2.

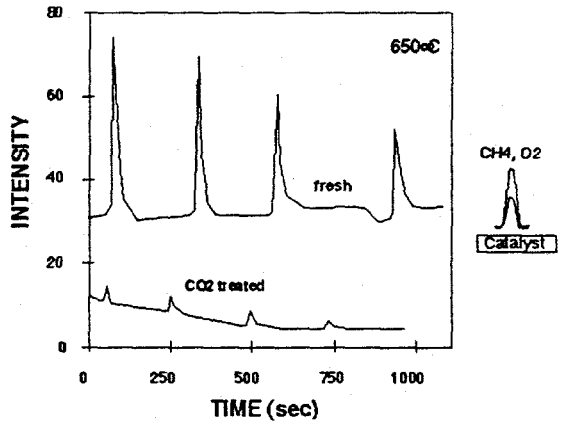

Figure 18. CO_2 signal during CH_4 and O_2 pulses on 2.5% $Li/LaNiO_3$, fresh and CO_2 treated at 650°C.

The lack of product detection during the pulse experiments, suggested that the pulses used were too small, and whatever C_2 products were formed, they were converted to CO_2 due to the large residence time of the pulse in the reactor. During steady state experiments, when C_2 products are detected, the amount of C_2 formed is large compared with the amount of catalysts, hence they are detected at the reactor outlet before they are converted to CO_2. To test this possibility, a step input of methane and oxygen was sent into the reactor at 700°C for two catalysts. One was a 2% Sr/La_2O_3 catalyst previously studied in our group (33) and the other was the 2.5% $Li/LaNiO_3$ catalyst. The results of experiments using a step input (not shown) show that both C_2 and CO_2 are detected by MS for both catalysts although the signals for the C_2 product (and methane conversion) is about six times smaller for the $Li/LaNiO_3$ catalyst than for the Sr/La_2O_3 catalyst. It follows that whatever C_2 products were produced on the Li promoted catalysts during the step experiments, they become converted to CO_2 that it is trapped on the catalyst surface. To further verify this possibility, pulses of ethane and oxygen were passed over the Li (1%) promoted and unpromoted $LaNiO_3$ catalysts.

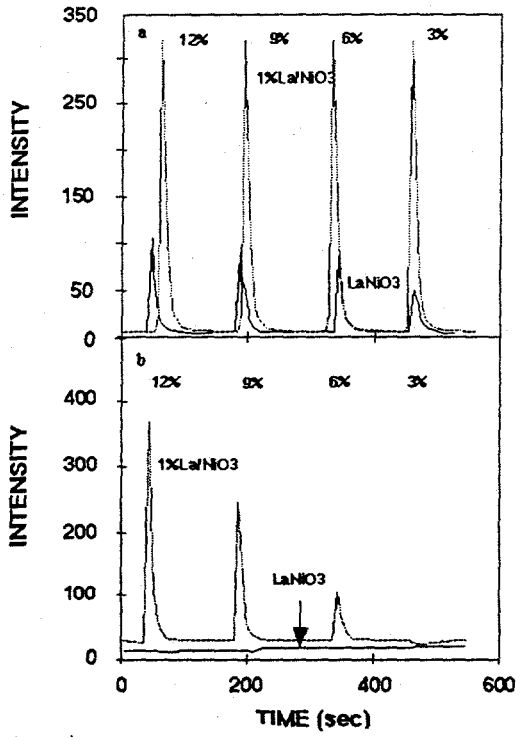

Figure 19. C_2H_6 and O_2 pulses with different O_2 concentration at 650°C.a- CO_2 signal, b- O_2 signal.

The CO_2 signal for ethane pulses with different oxygen concentration (fig. 19) is significantly larger for the unpromoted catalyst than for the promoted catalyst. The oxygen consumption in the unpromoted catalysts is 100% percent, indicating complete conversion of the C_2 products. In the 1% Li/$LaNiO_3$ catalysts, Li promotion significantly reduces the combustion of the reaction products. Isotopic oxygen tracing experiments were conducted in order to determine the effect of Li on the catalyst ability to exchange its lattice oxygen with the oxygen available in the gas-phase. Figure 20 shows the intensity signals at m/e 32, 34, and 36 when a step of $^{18}O_2$ in a He carrier stream was introduced into the reactor at 700°C. The results for the unpromoted catalysts show the appearance of a large peak of $^{16}O_2$ and the disappearance of the $^{18}O_2$ signal and subsequent recovery to the feed level. This demonstrates that isotopic oxygen exchanges rapidly with the oxygen from the lattice. The formation of the scrambled $^{16}O^{18}O$ oxygen goes through a maximum as the amount of ^{16}O is depleted within the solid. The same experiment is presented in the bottom half of fig. 20 for a heavily loaded Li catalyst to ascertain with better accuracy the effect of Li on the O_2 exchange. In this case the exchange, although qualitatively similar, is significantly reduced. This indicates that only a fraction of oxygen can exchange in the Li promoted catalyst due to the blockage of the sites for oxygen exchange or alternatively due to the diffusion of Li into the catalyst. This effect is probably linked to the suppression of the combustion activity with Li loading.

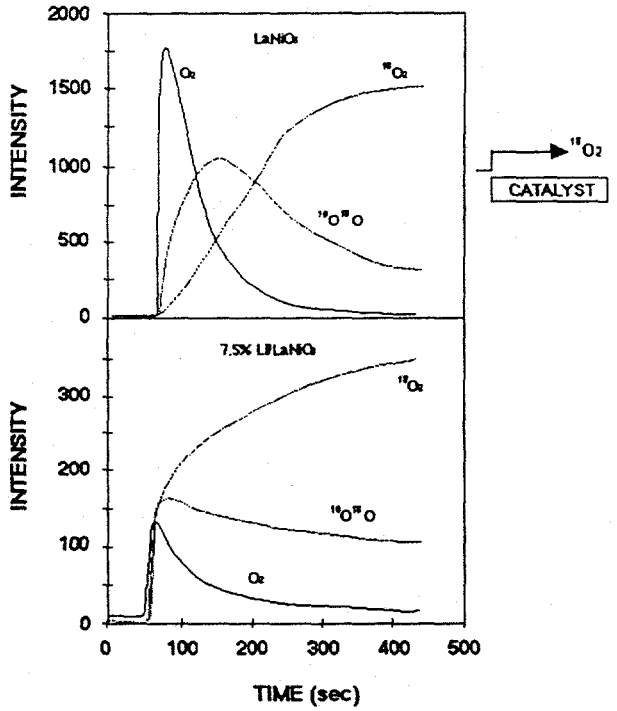

Figure 20. $^{18}O_2$ isotopic exchange at 700°C on $LaNiO_3$ and 7.5% Li/$LaNiO_3$.

A temperature programmed isotopic exchange experiment (TPIE) permits to ascertain the effect of temperature on the rate of oxygen exchange. In this case isotopic oxygen is exchanged first with catalysts at high temperature and then the reactor is cooled down to room temperature. The oxygen incorporated in the catalyst is the isotopic oxygen. A step of normal oxygen is passed over the catalyst while the temperature is increased. The appearance of the isotopes indicates the temperature at which exchange between catalyst and gas phase oxygen starts occurring. Fig. 21 displays results for the unpromoted and a 1% Li promoted catalysts. Oxygen exchange starts taking place at temperatures as low as about 325-340°C, which agrees with previous results on La_2O_3 (32). However, in the case of the 1%Li/$LaNiO_3$ catalyst O_2 exchange occurs at a slightly higher temperature that in case of the unpromoted catalyst. This effect is different than the results found during the promotion of La_2O_3 with Sr (32). In the

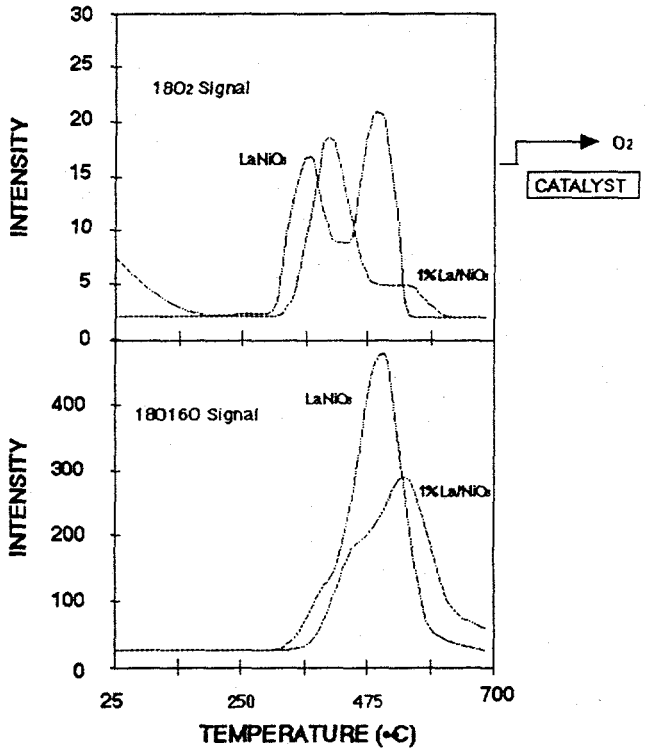

Figure 21. $^{18}O_2$ and $^{18}O^{16}O$ signals during TPIE experiment with oxygen.

later case Sr promotion lowered the temperature for oxygen exchange due to the increase of oxygen mobility and by the formation of oxygen vacancies. Furthermore, the shape of the oxygen exchange curve is different when Li is added to the catalysts with the disappearance of the higher temperature peak for the ^{18}O signal. It follows that there are two types of sites for oxygen exchange in these catalysts and Li promotion suppresses one of them. This finding agrees with the results for oxygen exchange at 700°C on the 7.5%Li promoted catalyst. The TPIE results show more specifically that Li promotion suppresses the high temperature sites for the oxygen exchange. Since Li promotion results in higher C_2 selectivity due to the

decrease in C_2 product combustion, it can be concluded that Li promotion blocks the higher temperature oxygen exchange sites which are presumably associated with C_2 product combustion.

To ascertain the extent of the methane surface interaction, isotopic switch experiment were conducted. In these experiments, described in detail elsewhere (60,61), a feed containing $^{13}CH_4$ and oxygen is switched with a feed containing a similar concentration of normal methane and oxygen. A trace of an inert Ar is also used to measure the transient response of a system in which no surface interaction occurs. The virtue of this method is that the surface remains under steady state conditions while the transient response of the isotopes can be

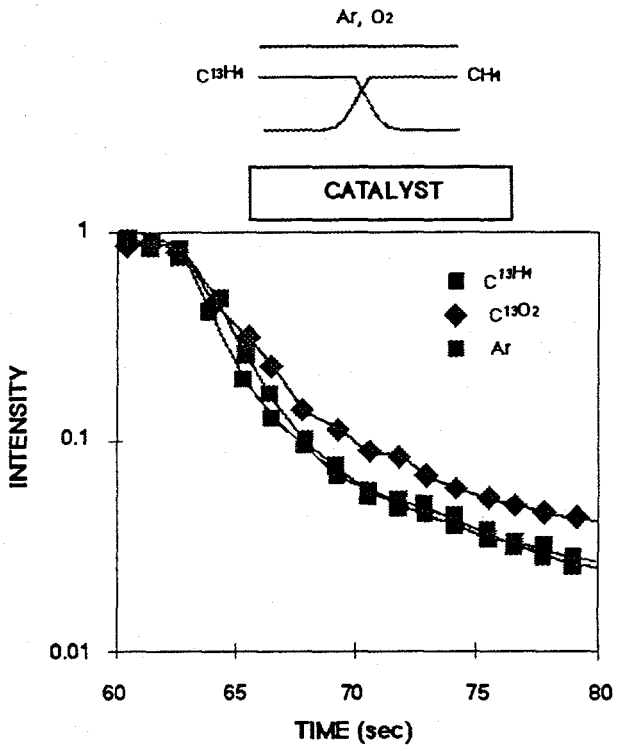

Figure 22. Methane 13 isotopic switch in the presence of Ar and oxygen on LaNiO3 catalyst at 650°C.

measured. The results of the switch experiments presented in fig. 22 for the unpromoted catalyst, show that the response of the $^{13}CH_4$ trace cannot be distinguished from that of Ar. Consequently, within the time resolution of this experiments the interaction of methane and the surface is too fast and cannot be distinguished from that of the inert gas such as argon. The $^{13}CO_2$ response observed during the methane switch experiment is also presented. It can be seen that this signal experiences a measurable delay with respect to that of Ar signal indicating that there is surface interaction leading to this delay. This indicates the formation of a surface species which retards the evolution of CO_2 with respect to Ar.

group, which measured adsorption of methane on the Sm_2O_3 oxide, suggested that methane acts as a weak acid, while the catalyst acts as a strong base. On the basis of the isotopic experiments, these authors concluded that adsorbed methane does not take part in the oxidative coupling reaction. On the other hand, Hatano and Otsuka presented evidence, that in the case of lithium nickelate, oxidative dimerization of methane proceeds through the dissociation of methane on the catalyst surface. Results of the experiment presented in fig. 22 suggest that for the $LaNiO_3$ catalyst and under reaction conditions applied in this study, the concentration of the long-lived methane species is too low to be differentiated with this technique from the interaction with argon over the surface of the catalyst.

SUMMARY OF SECTION 7-2.

Studies on double oxides of metals (Co, Ni and Rh) and lanthana, demonstrated that in fact the combination of these two catalytic functions yielded catalysts that operated at lower temperatures. The C_2 selectivity during the oxidative coupling of methane was relatively poor, unless Li was used as a promoter. $LaNiO_3$ in particular, was more selective than the other two metal oxides, hence the oxidative coupling of methane was studied on $Li/LaNiO_3$ catalysts using transient techniques. The results showed that Li promotion of $LaNiO_3$ metallo oxide significantly changes the catalytic properties of this compound. Steady state results indicate that the unpromoted catalyst oxidizes methane at temperatures significantly lower than those used during oxidative coupling. After Li promotion, the selectivity towards C_2 products increased from 2% up to 75% at 750°C for the 5% Li promoted catalyst. The increase in selectivity was achieved, however, at the expense of higher temperatures hence the intended low temperature reactivity was not realized in the Li promoted catalysts. Transient experiments indicate that lattice oxygen participates in the process of abstracting a hydrogen atom from the methane molecule. Isotopic exchange experiments conducted on unpromoted and Li promoted catalysts indicate that the presence of lithium significantly decreases the exchange capabilities of lanthanum nickel oxide by blocking oxygen exchange sites which may also be responsible for the total oxidation of methane. Methane 13 isotopic switch conducted over $LaNiO_3$ showed no detectable interaction with the surface of the catalyst under reaction conditions. The observed delay in the response of the $^{13}CO_2$ signal suggested that it can be considered as a secondary product and it is mainly formed from the combustion of C_2 hydrocarbons. While the transient studies conducted clearly revealed the role of Li, the yields attained in the Li promoted $LaNiO_3$ catalyst were similar to results reported for other Li promoted catalysts. Hence attention was directed to one outstanding result obtained, namely that the $LaRhO_3$ catalysts exhibited high selectivity to syngas production at relatively low temperatures.

7-3. METHANE PARTIAL OXIDATION TO SYNGAS OVER Rh CATALYSTS.

As it will be shown in this section the $LaCoO_3$, $LaNiO_3$ and $LaRhO_3$ catalysts exhibited very little selectivity to C_2 hydrocarbons yielding mainly CO_2 except for the Rh containing catalyst which was highly selective to CO and H_2. Hence the efforts in this section were directed to study the partial oxidation of methane on Rh catalysts.

CATALYST PREPARATION.

The $LaRhO_3$ catalyst was prepared in the same way as described above for the other metallo oxides. The supported Rh/TiO_2 catalyst was prepared by impregnation of Rh nitrate on TiO_2 using the dry impregnation technique until incipient wetness. The catalysts were dried in air at 100°C and calcined at 650°C in oxygen for two hours.

CATALYSTS CHARACTERIZATION.

X-ray diffraction

XRD patterns for the three metallo oxide catalysts show lines corresponding to the perovskite structures of the double oxides (not shown). The XRD patterns of the Li promoted catalyst show that there are significant changes in the major XRD lines of $LaNiO_3$ with the addition of small amount of Li, with additional lines characteristic for Li_2CO_3 . This behavior shows that the presence of lithium modifies the solid structure and its surface leading to C_2 selectivity improvement. When the improvement in the C_2 selectivity was not significant (i.e. Na promoted $LaCoO_3$) the XRD patterns consisted predominantly of the basic perovskite structure.

Surface area

The surface area for the $LaNiO_3$ phase was around 4.2 m^2/g, and after lithium promotion, the total surface area decreased to 2.9 m^2/g for the 1% Li promoted $LaNiO_3$. The decrease in the surface area after Li promotion can be explained by the formation of surface species such as Li carbonates and mixed oxides. In the case of the $LaCoO_3$ and $LaRhO_3$ catalysts, the BET results were in the range of 5-3 m^2/g with small changes observed after Li promotion.

ACTIVITY AND SELECTIVITY.

Methane and oxygen conversion versus temperature for the three unpromoted metallo-oxide catalysts are shown in fig. 23. It can be seen that the most active catalysts is $LaRhO_3$, followed by $LaNiO_3$ and $LaCoO_3$. It should be noted that the reaction starts at a much lower temperature than during methane oxidative coupling which agrees with the hypothesis that increasing the interaction of methane with the surface decreases the reaction temperature. Unfortunately, these catalysts are not selective for the production of C_2 hydrocarbons. Instead $LaNiO_3$ and $LaCoO_3$. only produce carbon dioxide whereas $LaRhO_3$ is 70% selective to CO production with the balance being CO_2. The method of catalyst preparation affected the selectivity. When using a stoichiometric mixture of La_2O_3 and CoO, the main product obtained at 700°C was CO_2 with only a 5% C_2 selectivity. However, in the perovskite $LaCoO_3$ catalyst, the C_2 selectivity was about 12%. It should be noted that La_2O_3 exhibits about 70% selectivity

under the same conditions, consequently the CoO acts as a combustion catalyst, and the formation of the perovskite structure decreases the concentration of the sites for total combustion. The effect of lithium on conversion, and product selectivity as a function of reaction temperature is presented in figure 24. In the catalyst reported below, referred as $Li/LaMO_3$, the level of Li loading was 2.5% Li by weight.

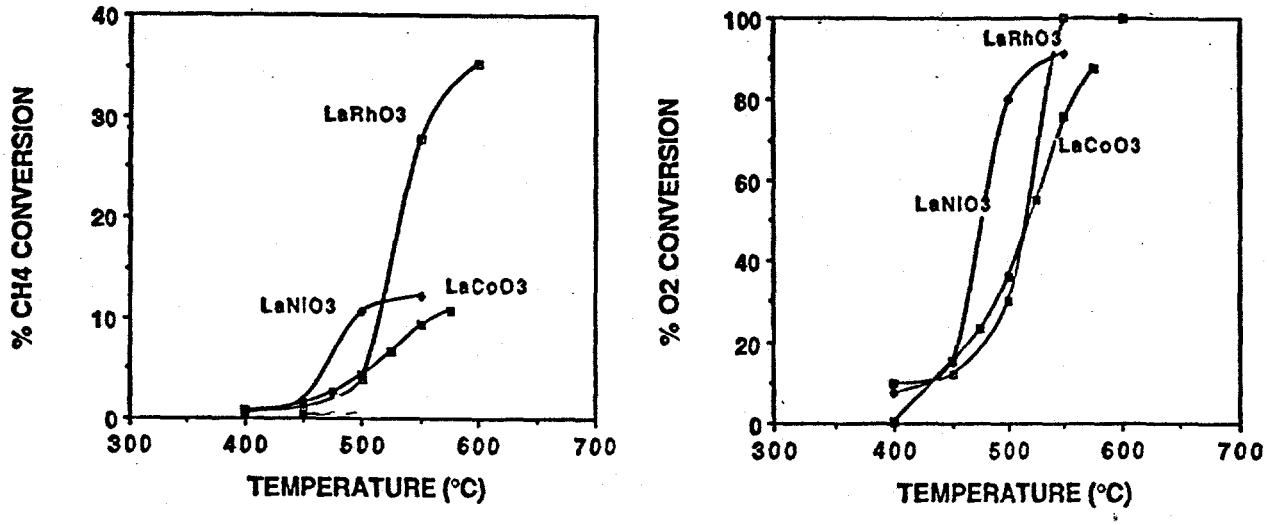

Figure 23. Methane and oxygen conversion versus temp. for $LaNiO_3$, $LaCoO_3$, $LaRhO_3$.

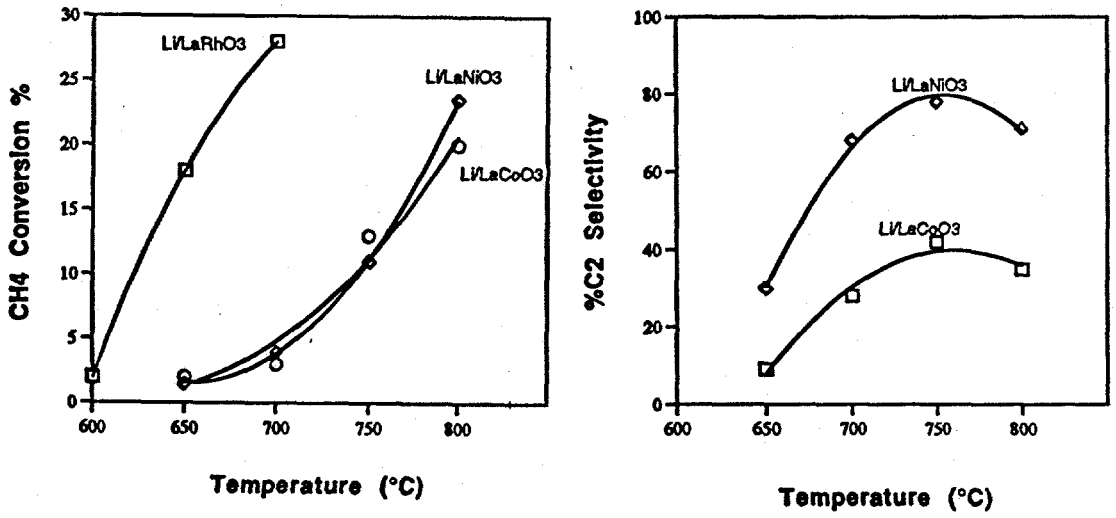

Figure 24. Methane conversion and C_2 selectivity for Li promoted catalysts.

Addition of the Li promoter shifts the reaction temperature to higher values, to a range typical for the methane oxidative coupling. For the $LaNiO_3$ and $LaCoO_3$ catalysts (700-800°C), and to about 625-675°C for the $LaRhO_3$ catalysts. These results indicate that Li promotion eliminates some of the very active sites present in the unpromoted catalyst, where methane-surface interaction occurs, and shifts the reaction to the classical free radical mechanism that predominates at high temperatures (58).

In the $Li/LaCoO_3$ catalyst the maximum C_2 selectivity reaches about 40% with the balance being CO_2 (fig. 24) . Promoting the $LaCoO_3$ catalyst with Na (not shown) resulted in a 20% C_2 selectivity at 750°C at a methane conversion of 18%. However, on the $Li/LaRhO_3$ catalysts the selectivity remains about the same as in the unpromoted catalyst, with no C_2 products being produced but with about 80% CO selectivity. The $Li/LaRhO_3$ catalyst also exhibits an ignition type behavior similar to the unpromoted perovskite with a steep increase in methane conversion from about 5% at 600°C to 30% at 650°C, at which point, the O_2 conversion reaches 100%.

The activity-selectivity results suggest that the reaction pathway on the metallo-oxide catalysts can be tuned up depending on the oxide and promoter used. The $LaNiO_3$ and $LaCoO_3$ catalysts are good total oxidation catalysts whereas the $LaRhO_3$ catalyst is a good catalyst for partial oxidation to synthesis gas. Li promotion turns the $LaNiO_3$ catalyst in a selective catalyst for oxidative coupling with some effect on $LaCoO_3$ and no effect on $LaRhO_3$.

Results of CO selectivity as a function of temperaure, presented in Fig.25, obtained at a CH_4/O_2 ratio of 300/8 show that the selectivity for CO increases with temperature whereas the CO_2 selectivity decreases as temperature increases, which is consistent with a mechanism in which CO_2 is the primary product. These results were obtained at low methane conversion (2%) for safety consideration since the mixture could reach the explosion limit. It was clear however that due to the low ignition temperature, higher concentrations of oxygen could be used. As the concentration of oxygen increased, the reaction ignited at about 400°C and the oxygen conversion reached 100% with 70-90% CO selectivity. The catalyst was ignited directly to a high conversion state (70-80% methane conversion) by starting with a methane rich mixture and increasing the oxygen concentration until ignition occurs. The $LaRhO_3$ catalyst yields high CO and H_2 selectivities in the high steady state. After ignition, the temperature increases steadily to about 600-700°C and remains at this level for the duration of the experiment. Following Schmidt and coworkers (31), we run the $LaRhO_3$ catalyst with methane oxygen mixtures without He diluent at flowrates of up to 500 cc/min .Without the diluent, the reaction becomes autothermal and no external heat source is required to sustain the partial oxidation reaction. It is necessary to operate at fast flows (>300-500 cc/min) to maintain the high CO selectivity and to keep the temperature of the catalyst below 700°C. Interestingly, after ignition, the conversion and selectivity become independent of flow rates in the low residence time regime.

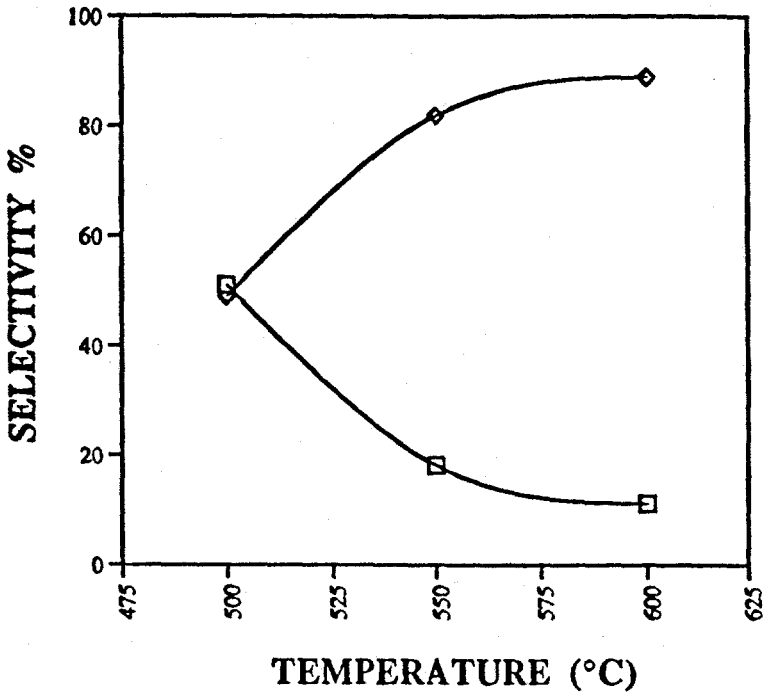

Figure 25 Selectivity for the $LaRhO_3$ catalysts.
[Diamond=CO selectivity, squares=CO_2 selectivity]

A Rh supported on titania catalyst was investigated now under the fast flow-millisec residence time conditions. The advantage of the Rh supported catalyst over the monolith Rh catalysts used by Hickman and Schmidt (31) is that it ignites at relatively low temperature (350°C) without the need for ammonia oxidation to ignite the methane reaction. Time on stream experiments using the fast flow catalyst indicates a fairly constant activity without significant deactivation for a period of 40 hrs.

The effect of catalyst flow rate in conversion and selectivity on the Rh/TiO_2 catalysts are presented in figure 26. It can be seen that high methane conversion and complete oxygen conversions with high CO and H_2 selectivity are attained in this fixed bed configuration. The residence time is in the order of a milliseconds indicating that this catalyst has high activity and selectivity. It should be noted that after ignition the reaction runs under autothermal conditions.

The fixed bed configuration, while safe due to the complete conversion of oxygen, present a potential hazards due to flame propagation in case a hot spot develops. For this reason a membrane reactor was developed to separate the methane and oxygen streams before contacting the catalyst. The membrane tube used is highly porous which permitted flowrates of the same order of magnitude as those used in a fixed bed, i.e. it permitted to operate at millisec residence time.

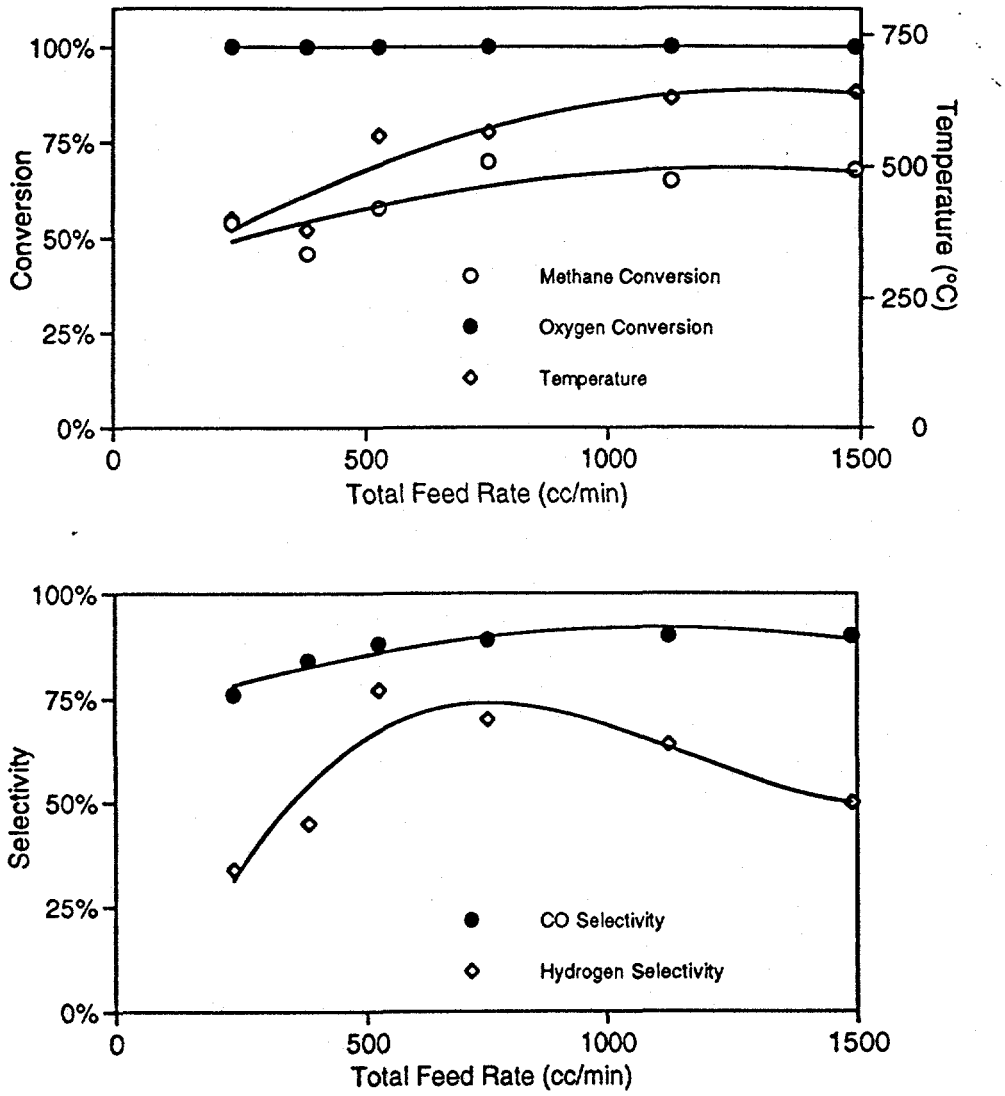

Figure 26. Conversion and selectivity versus total flow rate on a Rh/TiO_2 catalyst in a fixed bed reactor. Methane/oxygen ratio=2, 30 mg of catalysts, ignition temp. 320°C.

Results obtained in the membrane reactor are presented in figure 27 displaying methane conversion and CO and H_2 selectivity versus total feed rate. It can be seen that results as good and better as in the fixed bed configuration can be obtained in the membrane under similar fast flow conditions. These results have open up new possibilities of methane conversion since the

operation is now safe and it can be scaled up with minimum amounts of catalysts leading to high productivity.

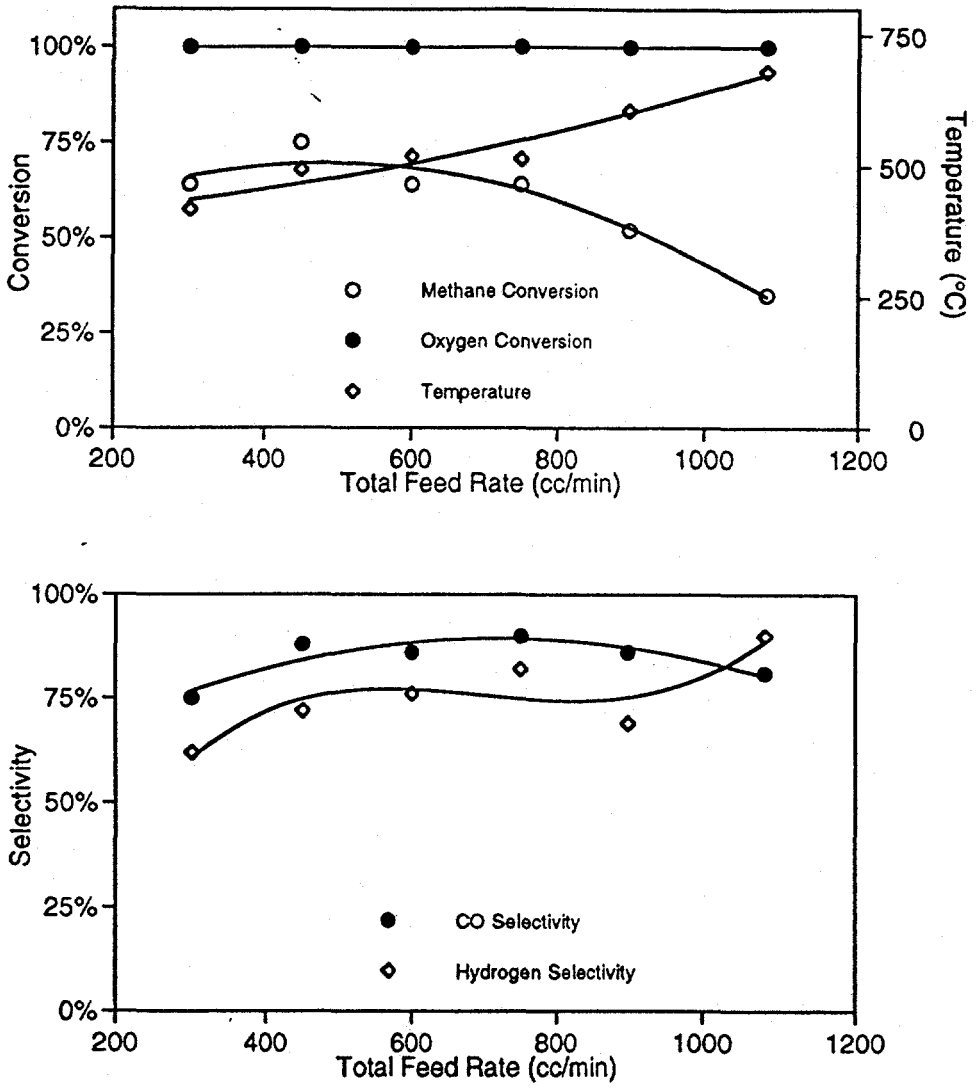

Figure 27. Methane and oxygen conversion versus residence time in a fast flow membrane reactor.

TRANSIENT STUDIES.

Pulses of methane diluted in helium with varying oxygen concentrations (8, 6, 4, 2%) were passed over 20 mg of the unpromoted and promoted Li/ $LaRhO_3$ catalysts at 650°C (Fig. 28). The left panel shows the signals for methane and oxygen (two pulses for each

concentration) and the right panel shows the signals for CO and CO_2 produced by these pulses. It can be seen that in all cases the only signal seen is CO_2 with minimum CO and no C_2 signal. Similar results were obtained for the unpromoted $LaRhO_3$, $LaNiO_3$ and $LaCoO_3$.

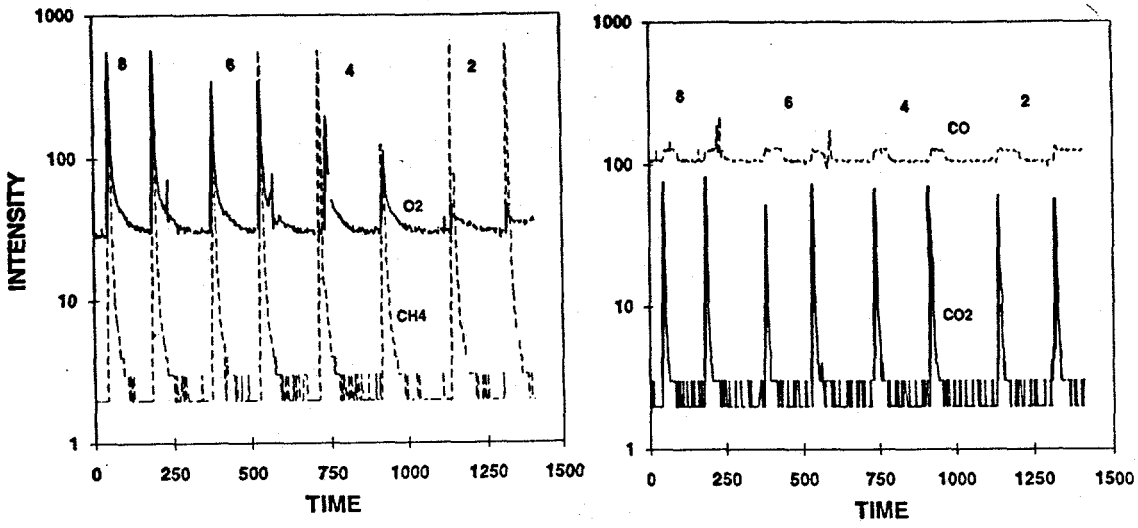

Figure 28. Pulses of CH_4/O_2 mixtures over the $Li/LaRhO_3$ catalyst.

The results of similar pulse experiments over a the $Li/LaNiO_3$ catalysts at 700°C presented in section 7-2, are quite different because they not only show that no C_2 are produced even though this catalyst is selective for C_2 production, but in addition in this case not even CO_2 is detected. This result shows that in the case of the $Li/LaNiO_3$ catalyst the species formed during these short pulses are captured by the surface of the catalyst probably as surface carbonates. Results of the pulse experiments in the $Li/LaCoO_3$ catalyst show an intermediate trend between the $Li/LaNiO_3$ and the unpromoted $LaCoO_3$ catalyst which agrees with its selectivity trends.

The pulse experiments clearly reflect the effect of Li on these surfaces and its correlation with the catalysts selectivity. In the case of the $Li/LaNiO_3$, the promoter alters the surface significantly eliminating the total combustion sites weakening or suppressing the interaction of methane with the surface and as a result the reaction pathway is displaced to the free radical mechanism (58). In addition isotopic oxygen exchange experiments show that presence of lithium significantly decreases the exchange capabilities of $LaNiO_3$ by blocking oxygen exchange sites which may also be responsible for the total oxidation of methane or the C_2 products formed . In the case of $LaRhO_3$, the most active catalyst, the main reaction product is

indeed CO_2. We speculate that in this case CO_2 reacts with methane via either the dry reforming reaction or via the reverse Boudouart reaction involving surface carbon to yield CO and H_2. The dry reforming mechanism has been proposed by Lunsford and coworkers (64) to explain the selectivity of Ba-Pb, Ba-Bi, and Ba-Sn perovskites, and the carbon reaction pathway has been proposed by Baerns and coworkers (65) for the partial oxidation of methane to synthesis gas on a 1% Rh/γ Al_2O_3 catalyst. The activity of La-M-O catalysts, with M=Co, Cr, Ni and Rh, for the partial oxidation of methane has also been reported (66). These authors reported that at 800°C synthesis gas yields near equilibrium were obtained on the La-Rh-O catalyst. The characterization results indicated that Rh was indeed in metal form due to a reduction procedure used initially used. Rh exhibits a unique CO selectivity behavior which is not related to its operation in a monolith substrate but rather due to the surface chemistry operating on this metal. Further work is underway in our laboratory to characterize determine the reaction pathway with a supported Rh catalyst that exhibits improved selectivity than the perovskite $LaRhO_3$ catalyst described in this paper.

SUMMARY FOR SECTION 7-3

Early results showed that the unpromoted $LaNiO_3$ and $LaCoO_3$ are good total oxidation catalysts whereas the $LaRhO_3$ is a good partial oxidation catalyst for synthesis gas production. Li promotion did not affect the selectivity of the $LaRhO_3$ catalyst which retained selective for syngas production even in the presence of Li. Furthermore this catalyst ignites to a high conversion state in an undiluted methane-oxygen feed at relatively low temperatures. This allowed to study the reaction at low CH_4/O_2 ratios in a fixed bed reactor. *Studies of 3% Rh supported on TiO_2 showed that the ignition temperature was even lower than the $LaRhO_3$ catalysts. Furthermore, it was fund that the Rh/TiO_2 catalyst operated autothermally in an undiluted feed at millisec residence times.* ***These are in fact the most significant results of this work.*** These results lead to the development of a fast flow membrane reactor which by separating the methane and oxygen feeds, can be operated safely under these conditions. The results in the membrane reactor were similar or better than in the fixed bed studies. *These results have open up the possibility of converting methane to syngas in an autothermal mode at low temperature and using low reactor volumes. This process has a significant commercial potential and further scaling up studies must be conducted to realize this potential.*

8. CONCLUSIONS

The oxidative conversion of methane was studied in catalysts containing a metal oxide function and another oxygen bearing compound. The selectivity depended on the type of metal oxide, the second component, and the promoter used. The reaction pathway could be directed towards the partial oxidation of methane to formaldehyde, to C_2 hydrocarbons or to syngas production. The conclusions for each pathway are presented separately.

The first catalytic system selected was the partial oxidation of methane to formaldehyde on VPO catalysts. The conversion and selectivity obtained with the Li-VPO catalyst are similar to those previously reported for other catalysts. The catalytic results clearly show that the Li cation improves the FA selectivity on VPO phases. It is also evident that the method used to add the Li^+ strongly influences the catalytic behavior. In order to obtain an active and selective catalyst, Li^+ has to be intercalated between the layers of the $VOPO_4*2H_2O$ which upon calcination forms the active phase. While the results regarding the role of Li could be significant in designing other catalyst for this reaction, the Li/VPO catalyst exhibited the type of low selectivity at low conversion characteristic of other catalyst reported in the literature. For this reason no further studies of this reaction pathway was conducted, and attention was focused on the oxidative coupling reaction.

Studies on double oxides of metals (Co, Ni and Rh) and lanthana, demonstrated that in fact the combination of these two catalytic functions yielded catalysts that operated at lower temperatures. The C_2 selectivity during the oxidative coupling of methane was relatively poor, unless Li was used as a promoter. $LaNiO_3$ in particular, was more selective than the other two metal oxides, hence the oxidative coupling of methane was studied on $Li/LaNiO_3$ catalysts using transient techniques. The results showed that Li promotion of $LaNiO_3$ metallo oxide significantly changes the catalytic activity of this compound. Steady state results indicate that unpromoted catalyst oxidizes methane at temperatures significantly lower than those used during oxidative coupling. After Li promotion the selectivity towards C_2 products increased from 2% up to 75% at 750°C for the 5% Li promoted catalyst. The increase in selectivity was achieved, however, at the expense of higher temperatures, hence the intended low temperature reactivity was not realized in the Li promoted catalysts. Transient experiments indicate that lattice oxygen participates in the process of abstracting a hydrogen atom from the methane molecule. Isotopic exchange experiments conducted on unpromoted and Li promoted catalysts indicate that presence of lithium significantly decreases the oxygen exchange capabilities of lanthanum nickel oxide by blocking oxygen exchange sites which may also be responsible for the total oxidation of methane. Methane 13 isotopic switch conducted over $LaNiO_3$ showed no detectable interaction with the surface of the catalyst under reaction conditions. The observed delay in the response of the $^{13}CO_2$ signal suggested that it can be considered as a secondary product and it is mainly formed from the combustion of C_2 hydrocarbons. While the transient

studies conducted clearly revealed the role of Li, the yields attained in the Li promoted $LaNiO_3$ catalyst were similar to results reported for other Li promoted catalysts. Hence attention was directed to one the outstanding result obtained, namely that the $LaRhO_3$ catalysts exhibited high selectivity to syngas production at relatively low temperatures.

Initial results showed that the unpromoted $LaNiO_3$ and $LaCoO_3$ are good total oxidation catalysts whereas the $LaRhO_3$ is a good partial oxidation catalyst for synthesis gas production. Li promotion did not affect the selectivity of the $LaRhO_3$ catalyst which retained high selective for syngas production even in the presence of Li. Furthermore this catalyst ignites to a high conversion state in an undiluted methane-oxygen feed at relatively low temperatures. This allowed to study the reaction at low CH_4/O_2 ratios in a fixed bed reactor. *Studies of 3% Rh supported on TiO_2 showed that the ignition temperature was even lower than the $LaRhO_3$ catalysts. Furthermore, it was fund that the Rh/TiO_2 catalyst operated autothermally in an undiluted feed at millisec residence times.* ***These are in fact the most significant results of this work.*** These results lead to the development of a fast flow membrane reactor which by separating the methane and oxygen feeds, can be operated safely under low CH_4/O_2 conditions. The results in the membrane reactor were similar or better than in the fixed bed studies. *These results have open up the possibility of converting methane to syngas in an autothermal mode at low temperature and using low reactor volumes. This process has a significant commercial potential and further scaling up studies must be conducted to exploit this potential.*

ACKNOWLEDGMENTS AND LIST OF PUBLICATIONS RESULTING FROM THIS GRANT

The author thanks Prof. J.L.G. Fierro and E. Pardo for of the ICP, SPAIN, for recording the XPS spectra. The results in section 6-1 were obtained by Dr. Manuel Lopez Granados who was partially supported by the Ministerio de Educación y Ciencia (Spain). The work in section 6-2 was carried by Dr. Z. Kalenik whose support was financed by this grant. The work in section 3 was carried in part by Dr. Kalenik and in part by Mr. M. Allibrando. The following papers have been written acknowledging funding from this grant.

1. "Partial oxidation of methane to formaldehyde by lithium promoted VPO catalyst", M. Lopez Granados and E.E. Wolf, **Applied Catal. A**, 131, 263-281 (1995).
2. "Transient studies of methane oxidative coupling over Li promoted $LaNiO_3$ catalysts" in *Methane and Alkane Conversion Chemistry*, Bhasin and Slocum (edits.), p.143, Plenum Press, 1995.
3. "Methane conversion on metallo-oxide catalysts", *Natural Gas Conversion International Meeting*, Kruger Park, South Africa, 1995, In press.
4. "Partial oxidation of methane to syngas in a millisec membrane reactor", M. Allibrando and E.E. Wolf, submitted, Catal. Lett.

9. REFERENCES

1. Pitchai, R. and Klier, K., Catal. Rev.-Sci. Eng., **28**, 13, (1986).
2. *Direct Methane Conversion by Oxidative Processes.* Edited by E. E. Wolf. Van Nostrand Reinhold Catalysis Series, New York , 1991.
3. Fox III, J.M., Catal. Rev.-Sci. Eng., **35**, 169, (1993).
4. Lee, J.S. and Oyama, S.T., Catal. Rev.-Sci. Eng., **30**, 249, (1988).
5. Spencer, N.D., J. Catal., **109**, 187, (1988).
6. Spencer, N.D., Pereira, C.J. and Grasselli, R.K., J. Catal., **126**, 546, (1990).
7. Smith, M.R., Zhang, L., Driscoll, S.A. and Ozkan, U.S., Catal. Letters, **19**, 1, (1993).
8. Bañares, M.A., Fierro, J.L.G. and Moffat, J.B., J. Catal., **142**, 406, (1993).
9. Spencer, N.D. and Pereira, C.J., J. Catal. **116**, 399, (1989).
10. Solymosy, F., Tombacz, I. and Kutzan, G., J. Chem. Soc. Chem. Commun., 1455, (1985).
11. Otsuka, K. and Hatano, M., J. Catal., **108**, 252, (1987).
12. Amir-Ebrahini, V. and Rooney, J.J., J. Mol Catal., **50**, L17, (1989).
13. Weng, T. and Wolf, E.E., Appl. Catal, **96**, 383, (1993).
14. Bordes, E., Catal. Today, **1**, 499, (1987).
15. Ohno, T. and Moffat, J.B., Catal Letters, **16**, 181, (1992).
16. Bordes, E., Courtine, P. and Pannetier, G., Ann. Chim. Paris, **8**, 105, (1973).
17. Antonio, M.R., Barbour, R.L. and Blum, P.R., Inorg. Chem., **26**, 1235,(1987).
18. Gopal, R. and Calvo, C., J. Solid State Chem., **5**, 432, (1972).
19. Tachez, M., Théobald, F. and Bordes, E., J. Solid State Chem., **40**, 280, (1981).
20. Ladwig, G., Z. Anorg. Allg. Chem., **338**, 266, (1965).
21. Mars, P., and van Krevelen, D. W., *Chem. Eng. Sci.,* Suppl. **3**, 4 (1954).
22. Otsuka, K., Jinno, K., *Inorg. Chim. Acta*, **121**, 233 (1986).
23. Otsuka, K., *Inorg. Chim. Acta*, **132**, 123 (1987).
24. Ito, T., Wang, J.-X Lin, C.-H and Lunsford, J. H., *J. Chem. Soc.,* **107**, 5062 (1985).
25. Driscoll, D. J., Campbell, K. D., and Lusford, J. H., *Adv. Catal.,* **35**, 139 (1987).
26. Lane, G. S., and Wolf, E. E., *J. Catal.* **113**, 144 (1988).
27. Ashcorft, P.T., Cheetham, A.K., Foord, J.S., Gree, M.L., Grey, C.P., Murrel, A.J., and Vernon, P.D.F., *Nature* , **344**, 319 (1990).
28. Lane, G. S., Miro, E. E., and Wolf, E. E., *J. Catal.,* **119**, 161 (1988).
29. Lane, G. S., and Wolf, E. E., *Proc. Ninth Int. Congress Catal.*, Calgary, Canada ,1988.
30. De Boy, J. M., and Hicks, R. F., *J. Chem. Soc., Chem. Commun.* 982, (1988).
31. Hickman, D.A., and Schmidt, L.D., *J.Catal.*,**138**, 267 (1992).
32. Kalenik, Z., and Wolf, E. E., *Catal. Lett.* **11**, 309 (1991).
33. Kalenik, Z., and Wolf, E. E., *Catal. Lett..* **9**, 441 (1991).
34. Johnson, J.W. and Jacobson, A.J., Angew. Chem. Int. (Ed. Eng.), **22**, 412, (1983).

35. Chauvel, B., Bondot, P., de Roy, M. and Besse, J.P., Mater. Res. Bull., **26**, 487, (1991).
36. Bhargava, R.N. and Condrate, R.A. Sr., Appl. Spectroscopy, **31**, 230, (1977).
37. Stranford, G.T. and Condrate, R.A. Sr., Spectroscopy Letters, **17**, 85, (1984).
38. Martínez Lara, M., Jiménez López, A., Moreno Real, L., Bruque, S., Casal, B. and Ruiz-Hitzky, E., Mater. Res. Bull., **20**, 549, (1985).
39. Bond, G.C. and Flamerz Tahir, S., Appl. Catal., **71**, 1, (1991).
40. Meyers, G.F., Hall, M.B., Chinn, J.W. Jr. and Lagow, R.J., J. Am. Chem. Soc., **107**, 1413, (1985).
41. Matsumura, Y., Hashimoto, K. and Moffat, J.B., Catal. Letters, **13**, 283, (1992).
42. Sun, Q., Herman, R.G. and Klier. K., Catal. Letter, **16**, 251, (1992).
43. Parmaliana, A., Frusteri, F., Mezzapica, A., Miceli, D., Scurrell, M.S. and Giordano, N., J. Catal., **143**, 262, (1993).
44. Martínez Lara, M., Moreno Real, R., Pozas Tormo, R., Jiménez Real, A., Ruiz, P. and Poncelet, G., Can. J. Chem., **70**, 5, (1992).
45. Kang, H.Y., Wang, S.L. and Lii, K.H., Acta Crystallogr., Sect. C., **48**, 975, (1992).
46. Kang, H.Y., Wang, S.L., Tsai, P.P. and Lii, K.H., J. Chem. Soc. Dalton Trans., 1525, (1993).
47. Liu, H.-F., Liu, R.-S., Liew, K.Y., Johnson, R.E. and Lunsford, J.H., J. Am. Chem. Soc., **106**, 4117, (1984).
48. Barbaux, Y., Elamrani, A. and Bonnelle, J.P., Catal. Today, 1, 147, (1987).
49. Smith, M.R. and Ozkan, U.S., J. Catal.., **141**, 124, (1993).
50. Smith, M.R. and Ozkan, U.S., J. Catal., **142**, 226, (1993).
51. Yto, T., Wang, J.-X., Lin, C.-H. and Lunsford, J.H., J. Am. Chem. Soc., **107**, 5062 (1985).
52. Tong, Y. and Lunsford, J.H., J. Am. Chem. Soc., **113**, 4741, (1991).
53. Lin, C.-H., Ito, T., Wang, J.-X. and Lunsford, J.H., J. Am. Chem. Soc., **109**, 4808, (1987).
54. Lin, C.-H., Wang, J.-X. and Lunsford, J.H., J. Catal., **111**, 317, (1988).
55. Zhang, H.-S., Wang, J.-X., Driscoll, D.J., and Lunsford, J.H., J. Catal., **112**, 366, (1988).
56. Wu, M.-C., Truong, C.M., Coulter, K. and Goodman, D.W., J. Catal.,**140**, 344, (1993)
57. Handbook of Chemistry and Physiscs. 6th Edition. CRC Press. Florida, 1985.
58. Lunsford, J. H., In *Direct Methane Conversion by Oxidative Processes*. Edited by E. E. Wolf, Van Nostrand Reinhold Catalysis Series, p. 3, New York 1991.
59. Al-Ubaid, A., and Wolf, E. E., *Appl. Catal.*, **40**, 73 (1985).

60.Miro, E. E., Kalenik, Z., Santamaria, J., and Wolf, E. E., *Catalysis Today,* **6**, 511 (1990).

61.Peil, K. P., Marcelin, G., and Goodwin, J. G., In "*Direct Methane Conversion by Oxidative Processes*", Edited by E. E. Wolf. Van Nostrand Reinhold Catalysis Series, p. 138, New York 1991.

62. Ekstrom, A., Lapszewicz, J. A., *J. Chem. Soc. Chem. Commun.*, 797 (1988).

63. Hatano, M., and Otsuka, K., *J. Chem. Soc., Faraday Trans.* **I, 85** 2, 199 (1989).

64. Dissayanake, D., Kharas, K.C., Lunsford, and M. Rosynek, *J. Catal,* **139**, 652 (1993).

65. Buyevskaya, O.V., Wolf, D., and Baerns, M., *Catal. Lett.* **239**, 249 (1994).

66. Slagtern, Asa, Olsbye, U., *Appl. Catal. A. Gen.*, **110**, 99 (1994).

LIST OF TABLES

Page

Table 1 Assignments of the FTIR bands to vibration modes in the region (500-1500 cm^{-1}) for some of the unsupported samples. 18

Table 2. XPS intensity ratio I_{Li}/I_V for the Li1s and V2p3/2 peaks in the unsupported catalysts. 19

Table 3. Percentage of the different O_2 isotopes in the outlet (referred to the total oxygen present in the flow) after 4 min of $^{18}O_2$ exchange on various supported catalysts at 923 K. 20

LIST OF FIGURES

Page

Figure 1: Schematic diagram of the apparatus. 8

Figure 2: Schematic diagram of the membrane reactor. 10

figure 3. XRD diffraction pattern of VPO-u. 14

Figure 4a: FTIR spectra for several samples in the region 3750-2900 cm^{-1}. 15

Figure 4b. FTIR spectra for several samples in the region 1750-1550 cm^{-1}. 16

Figure 5: FTIR espectra for several unsupported samples in the region (1500-500 cm^{-1}). 17

Figure 6: CH_4 conversion (%) as a function of temperature for several unsupported catalysts (conditions as indicated in experimental section). 20

Figure 7: HCHO selectivity(%) as a function of CH_4 conversion(%) for the same catalysts of fig. 6. 21

Figure 8: CH_4 conversion (%) as a function of temperature for several supported catalysts (conditions as indicated in experimental section). 21

Figure 9: HCHO selectivity(%) as a function of CH_4 conversion (%) for the same catalysts of fig.8. 22

Figure 10: Comparison of the HCHO selectivity vs CH_4 conversion curves in double bed and single bed configurations at two different flow rates (conditions as indicated in experimental section). 23

Figure 11. $^{18}O_2$, $^{16}O_2$ and $^{16}O^{18}O$ concentrations in the effluent when a $^{18}O_2$ step in He is fed through a Li-VPO/SiO_2 at 923 K. 24

Figure 12. XRD patterns of unpromoted and Li promoted $LaNiO_3$. 29

Figure 13. CH_4 conversion and C_2 selectivities vs reaction temperature during OC reaction at different Li loadings. 30

Figure 14. CH_4 conversion and C_2 selectivities vs reaction temperature on $LaNiO_3$ catalyst with different Ni/La ratio. 31
Figure 15. Pulses of methane over a $LaNiO_3$ catalsyst at 700°C 32
Figure 16. CH_4 pulses with different O2 concentration on $LaNiO_3$ at 550°C. 33
Figure 17. CH_4 pulses with different O2 concentration on 2.5% $Li/LaNiO_3$ at 700°C.
Figure 18. CO_2 signal during CH_4 and O_2 pulses on 2.5% $Li/LaNiO_3$, fresh and CO_2 treated at 650°C. 34
Figure 19. C_2H_6 and O_2 pulses with different O_2 concentration at 650°C.a- CO_2 signal, b- O_2 signal. 35
Figure 20. $^{18}O_2$ isotopic exchange at 700°C on $LaNiO_3$ and 7.5% $Li/LaNiO_3$. 36
Figure 21. $^{18}O_2$ and $^{16}O^{18}O$ signals during a TPIE experiment. 37
Figure 22.Methane 13 isotopic switch in the presence of Ar and oxygen on $LaNiO_3$ catalyst at 650°C. 38
Figure 23. Methane and oxygen conversion versus temp. for $LaNiO_3$, $LaCoO_3$, $LaRhO_3$. 41
Figure 24. Methane conversion and C_2 selectivity for Li promoted catalysts. 41
Figure 25. Selectivity for the $LaRhO_3$ catalysts. 43
Figure 26. Conversion and selectivity on a Rh/TiO_2 catalyst as a function of residence time. 44
Figure 27 Methane and oxygen conversion versus residence time in a fast flow membrane reactor. 45
Figure 28. Pulses of CH_4/O_2 mixtures over the $Li/LaRhO_3$ catalyst. 46